# Organization and Ontogeny of a Complex Lateral Line System in a Goby (Elacatinus lori), with a Consideration of Function and Ecology

Authors: Nickles, Katie R., Hu, Yinan, Majoris, John E., Buston, Peter M., and Webb, Jacqueline F.

Source: Copeia, 108(4) : 863-885

Published By: The American Society of Ichthyologists and Herpetologists

URL: https://doi.org/10.1643/CG-19-341

Copeia

Copeia 108, No. 4, 2020, 863–885

# Organization and Ontogeny of a Complex Lateral Line System in a Goby (*Elacatinus lori*), with a Consideration of Function and Ecology

Katie R. Nickles[1], Yinan Hu[1,2], John E. Majoris[3,4], Peter M. Buston[3], and Jacqueline F. Webb[1]

**Gobies (family Gobiidae) have a complex mechanosensory lateral line system characterized by reduced lateral line canals and a dramatic proliferation of small superficial neuromasts (on ''sensory papillae''), which are arranged in lines on the head, trunk, and tail. A suite of morphological methods was used to describe the distribution and morphology of canal and superficial neuromasts in the neon goby, *Elacatinus lori*, and to describe the ontogeny of the lateral line system for the first time for any gobiiform fish. Portions of only three cranial lateral line canals are retained and they contain a total of eight canal neuromasts. In addition, 128–155 superficial neuromasts are found in six head series (comprising 33 neuromast lines or rows). Superficial neuromasts are found in one body series (65–80 neuromasts arranged in three groups of vertical lines or ''stitches'') and one caudal fin series (3 lines, each located between fin rays and comprised of many small neuromasts; total of 27–53 neuromasts) extending to the tip of the caudal fin. The general distribution of neuromasts is established early during the larval stage, and neuromast numbers increase within and among lines resulting in an increase in overall complexity of the system. On day-of-hatch, a total of 22 neuromasts are present. At ~15 days post-hatch, all eight cranial canal neuromasts are present, and, in post-settlement juveniles (''settlers''), they are enclosed in canals and a total of ~185 neuromasts are found on the head, trunk, and tail. All neuromasts are small (~40 μm long) and diamond-shaped, but three subpopulations (canal neuromasts, canal neuromast homologs, superficial neuromasts) are defined based on their location and their arrangement within lines (''tip-to-tip'' or ''side-by-side''). The ontogeny of the lateral line system and distinctions among neuromast subpopulations help to reveal the structural and functional organization of the complex lateral line system in *Elacatinus* and will contribute to the interpretation of neuromast patterns in other gobiiforms. A comparison of superficial neuromast number in 12 species of *Elacatinus* and *Tigrigobius* (sister genera) revealed variation among species that live in different reef microhabitats, which suggests that adaptive evolution in the lateral line system is evident among closely related taxa.**

GOBIIFORMES is one of the most species-rich orders of fishes (>2,000 species; Patzner et al., 2011; Nelson et al., 2016). Fishes in the family Gobiidae (gobies, ~1359 spp.) are the most species-rich family on coral reefs, with some temperate and freshwater representatives (Nelson et al., 2016). They are characterized by a combination of reductive (paedomorphic) and constructive (peramorphic) features: 1) partial or complete reduction of some or all of the cranial lateral line canals typically found in bony fishes (*sensu* Webb, 2014a; Miller and Wongrat, 1979; Birdsong and Robins, 1995), 2) the absence of the trunk canal (Ahnelt et al., 2004), and 3) a dramatic proliferation of hundreds or even thousands of superficial neuromasts that sit on top of "sensory papillae," which are organized in lines or rows (Wongrat and Miller, 1991) on the head, trunk, and tail. The number and distribution of lateral line canal pores, and of the sensory papillae in particular, have been used as characters for taxonomic and systematic studies of gobiiforms (e.g., Sanzo, 1911; Takagi, 1957, 1988; Akihito, 1986; Wongrat and Miller, 1991; Gill and Bradley, 1992; Mennesson et al., 2019). However, the lateral line system of only a small fraction of gobiiforms, and of gobiids in particular, has been studied in any detail.

Vital fluorescent imaging is now being used to describe the distribution and innervation of canal and superficial neuromasts, and their numbers vary dramatically among the few gobioids examined (Asaoka et al., 2011, 2012, 2014). For instance, *Rhyacichthys aspro* (family Rhyacichthyidae, a basal gobioid family, as defined by Thacker, 2009) retains seven cranial canals (including the infraorbital, mandibular) and a trunk canal containing a total of 227 canal neuromasts (Larson, 2011). In addition, 308 superficial neuromasts are found on the skin on one side of the head, body, and tail (Asaoka et al., 2014). In contrast, *Glossogobius olivaceus* (family Gobiidae) retains portions of only three of the cranial canals typical of bony fishes (supraorbital, preopercular, postotic). Those canals contain only nine canal neuromasts, but 4,828 superficial neuromasts are found on the skin of the head, body, and tail (Asaoka et al., 2012).

The proliferation of superficial neuromasts is also known in other gobiiform taxa (apogonids, Bergman, 2004; Sato et al., 2017, 2019; kurtids, Thacker, 2009), as well as in cyprinids (Beckmann et al., 2010; Schmitz et al., 2014), characids (neon tetras and allies, Yoshizawa et al., 2010, 2014; unpubl. data), and other taxa that occupy hydrodynamically quiet and/or light-limited marine and freshwater habitats (e.g., stomiiforms and other deep-sea fishes, Marranzino and Webb, 2018; cavefishes, Montgomery et al., 2001; Poulson, 2001; Soares and Neimiller, 2013; Yoshizawa et al., 2014; Jiang et al., 2016; Neimiller et al., 2019).

The adaptive significance of superficial neuromast proliferations on the skin of taxonomically and ecologically

[1] Department of Biological Sciences, University of Rhode Island, 120 Flagg Road, Kingston, Rhode Island 02881; Email: (JFW) Jacqueline_webb@uri.edu. Send reprint requests to JFW.
[2] Department of Biology, 355 Higgins Hall, Boston College, Chestnut Hill, Massachusetts 02476.
[3] Department of Biology and Marine Program, Boston University, 5 Cummington Street, Boston, Massachusetts 02215.
[4] Red Sea Research Center, King Abdullah University of Science and Technology, Thuwal 23955-6900, Saudi Arabia.
Submitted: 12 December 2019. Accepted: 4 August 2020. Associate Editor: M. P. Davis.
 DOI: 10.1643/CG-19-341 Published online: 18 December 2020

diverse fishes is presumably related to the increased sensitivity of the superficial neuromasts to the velocity component of local water flows (as opposed to the acceleration component to which canal neuromasts respond; Denton and Gray, 1989). The presence of a relatively high number of closely spaced superficial neuromasts would also presumably increase their ability to respond to local, small scale water flows at higher spatial resolution (e.g., Montgomery and Milton, 1993; Yoshizawa et al., 2010). However, adaptive evolution of the lateral line system among gobies has been addressed in only a few instances (e.g., Ahnelt et al., 2004; Asaoka et al., 2014). An ontogenetic approach would likely reveal the origin and evolution of the complex superficial neuromast patterns in gobies, but their post-embryonic development is known from only a few studies (e.g., Tavolga, 1950; Feddern, 1967; Valenti, 1972; Meirelles et al., 2009), and only a handful have included any mention of the lateral line system (the sensory papillae; Konagai and Rimmer, 1985; Ahnelt and Scattolin, 2003; Ahnelt et al., 2004).

The Line Snout Goby, *Elacatinus lori*, is a sponge-dwelling neon goby endemic to Belizean reefs (D'Aloia et al., 2011). It is relatively easy to locate, collect, and study in the field (Majoris et al., 2018a) and can be reared and studied in the laboratory (Majoris et al., 2018b). For these reasons, it has been developed as a model for the first integrated analysis of larval dispersal and orientation behavior (D'Aloia et al., 2013, 2014, 2015, 2017, 2018, 2020; Lindo et al., 2016; Majoris et al., 2018a, 2019), and the development of the sensory systems thought to mediate this critical larval behavior (olfactory and gustatory systems, Hu et al., 2019; this study).

Gobies in *Elacatinus* and *Tigrigobius* (once considered a subgenus of *Elacatinus,* and not considered to be monophyletic; Ruber et al., 2003; Van Tassell, 2011; Huie et al., 2019) are members of the North American seven-spined gobies (family Gobiidae, tribe Gobiosomatini, Thacker and Roje, 2011). These fishes demonstrate diversity in feeding ecology and occupy different microhabitats (e.g., presumably characterized by different flow regimes) on coral reefs, which may provide the selection pressures driving the evolution of the lateral line system. *Elacatinus* is composed of at least 21 coral reef species (cryptic species are common; Van Tassell, 2011) and is comprised of three clades: a basal Pacific species, the sponge-dwelling planktivores (including *Elacatinus lori*), and the coral-dwelling cleaners (dedicated and facultative; Ruber et al., 2003; Taylor and Hellberg, 2005; Colin, 2010; Victor, 2014; Huie et al., 2019). *Tigrigobius* is composed of 12 coral reef species that occupy a more diverse set of microhabitats; it includes coral-dwelling facultative cleaners, sponge-dwellers, chiton burrowers, and urchin-associated species (Van Tassell, 2011; Huie et al., 2019). The lateral line system of neither *Elacatinus* nor *Tigrigobius* has been studied in detail, but the sensory papillae and cranial lateral line canal pores have been illustrated in a few instances (Fig. 1).

The goal of this study was to use a suite of morphological methods to: 1) describe neuromast distribution and morphology in *E. lori*, 2) determine how this pattern arises from day-of-hatch through settlement and transition to the juvenile stage, and 3) examine the relationship between neuromast number and microhabitat (feeding ecology) among species of *Elacatinus* and *Tigrigobius*.

## MATERIALS AND METHODS

***Material examined.***—Mated pairs of *Elacatinus colini* and *Elacatinus lori* were collected near Carrie Bow Caye, Belize (16°48′09″N, 88°04′55″W) and maintained in a flow-through seawater laboratory at the International Zoological Expeditions field station on South Water Caye, Belize (16°49′N, 88°05′W), or in a recirculating seawater system at Boston University, USA. Ontogenetic series of *E. colini* and *E. lori* were reared from hatch to settlement in Belize (Table 1) and were fed zooplankton. Majoris et al. (2018a) provides additional methodological detail. Additional wild-caught post-settlement *E. colini* and *E. lori* (WC settlers) were collected from reef habitats within the South Water Caye Marine Reserve. Fishes were immersed in cold seawater (2–4°C) for 2 min and then fixed in cold (2–4°C) 10% formalin in seawater (or in phosphate-buffered saline; PBS) for subsequent anatomical study, which is consistent with American Veterinary Medical Association guidelines on euthanasia of small warm-water fish (Boston University IACUC protocol #16-001). Care was taken to ensure that the fishes did not contact ice directly. Field research in Belize and the export of samples from Belize were carried out with the approval of the Belize Fisheries Department.

Museum specimens (American Museum of Natural History, AMNH; see Table 1) representing three species of *Elacatinus* and six species of *Tigrigobius* from different microhabitats were also available for study (coral-dwellers—*E. randalli*, *T. dilepis*, *T. inornatus*, *T. pallens*, and *T. zebrella*; sponge-dwellers—*E. horsti*; species occupying "other" microhabitats—*E. puncticulatus*, *T. gemmatus*, and *T. multifasciatus*).

***Vital fluorescent staining of neuromasts.***—A total of 23 live larvae of *Elacatinus lori* (0–38 dph [days post-hatch]; 3 mm notochordal length [NL]–9.5 mm standard length [SL]) reared in the Buston Lab at Boston University and wild caught adults ($n$ = 4, 42–62 mm SL) were used to visualize the number and distribution of canal and superficial neuromasts (Table 1). Fish were placed in 0.0024% 4-di-2-ASP (4-(4-diethylamino-styryl)-N-methylpyridinium iodide; Sigma Aldrich) in tank water for 5 minutes, rinsed in tank water, anaesthetized in 0.02% buffered MS-222 (Tricaine methanesulfonate; Sigma Aldrich), and pinned in a petri dish lined with silicone and containing additional MS-222 solution. Specimens were imaged on a Nikon SMZ 1500 dissecting scope equipped with epifluorescence (GFP filter set), a Spot digital camera (Model 25.22, Mp Color Mosaic), and Spot software (v.5.0; Diagnostic Instruments, Sterling Heights, MI).

Neuromast distribution maps were created using 29–130 fluorescent images per individual (for the smallest and largest fishes, respectively), and the number of neuromasts found on one side of the head, trunk, and tail were recorded. Some variation in neuromast number was noted within lines (or rows) among individuals of the same age, so composite maps were created using the mean number of neuromasts per line for all individuals of the same age. Additional neuromast maps derived from histological data (see below) were compared to maps based on fluorescent imaging and to published images of neuromast distributions in related taxa (Sanzo, 1911; Marshall, 1986; Hoese and Reader, 2001). The lines of neuromasts (also referred to as rows of sensory papillae in the literature) and the series in which they occur were then named as per Sanzo (1911) and Wongrat and

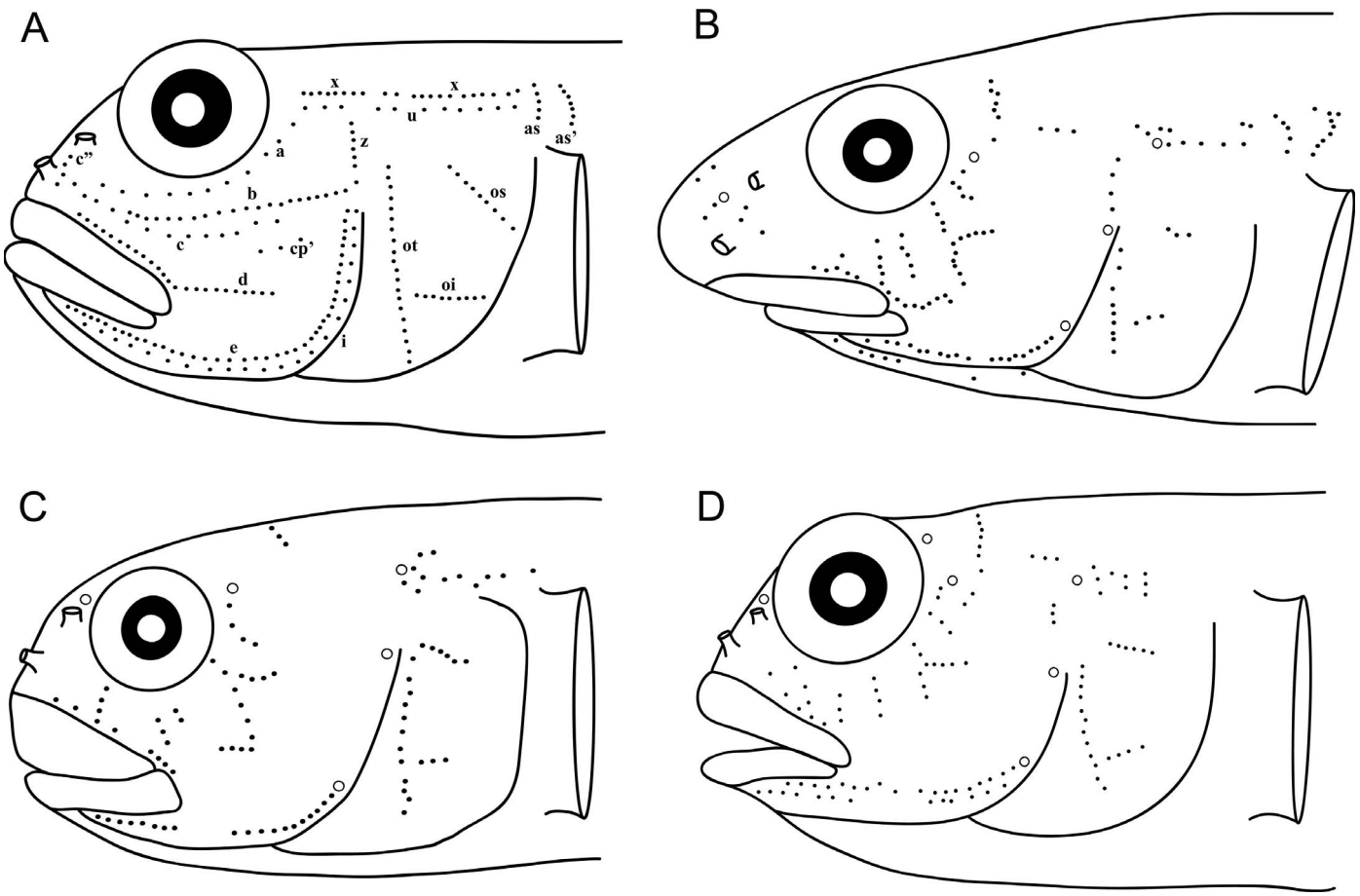


**Fig. 1.** Examples of the distribution of lateral line canal pores (open circles) and superficial neuromasts (filled circles) in longitudinal and transverse patterns in gobies. (A) *Thorogobius macrolepis* has a longitudinal pattern with lines ventral to the eye (lines a, b, c, and d) that extend rostro-caudally (re-drawn from Sanzo, 1911). (B) *Elacatinus oceanops* has a transverse pattern with lines ventral to the eye that radiate from the edge of the orbit, the site of the ancestral infraorbital canal (the only published data for *Elacatinus* spp.; re-drawn from Miller, 1972). (C) *Tigrigobius limbaughi* (=*Elacatinus limbaughi*), with a transverse pattern (re-drawn from Hoese and Reader, 2001). (D) *Tigrigobius macrodon*, with a transverse pattern (re-drawn from Miller, 1972).

Miller (1991). Neuromasts within a line were numbered from dorsal to ventral (vertical lines) or rostral to caudal (horizontal lines). Pores in the cranial canals were visualized in histological material and their identification was confirmed using SEM and μCT and named using terminology from Sanzo (1911).

***Histology.***—Histological material was used to visualize the cranial lateral line canals, canal pores, and neuromasts. This material (previously prepared; see Hu et al., 2019) comprised an ontogenetic series of *E. lori* reared in Belize ($n = 17$, 0–44 dph, 3 mm NL–11 mm SL, 2016) and a wild-caught settler ($n = 1$, 14 mm SL, 2015). Fixed fish > 6 mm SL were decalcified in Cal-Ex (Thermo Fisher Scientific) for 2 h (6–7.5 mm SL), 3.5 h (8–8.5 mm SL), or 7–8 h (>8.5 mm SL) and rinsed in PBS for 2 h. All fish were then dehydrated in an ascending ethanol series (to 95% ethanol) and infiltrated overnight in glycol methacrylate resin (GMA, Technovit 7100, Electron Microscopy Sciences). Individual fish were first embedded in small resin blocks and then 6–8 small resin blocks containing those fish were re-embedded in a single larger block of resin to allow sectioning in the transverse plane. Sections were cut at 5 μm thickness on a Leica 4M2265 motorized microtome with a tungsten carbide knife and individually mounted out of $dH_2O$ onto clean slides. Slides were air-dried overnight, stained with 0.5% aqueous cresyl violet for 5 min, rinsed in running tap water, air-dried overnight, and coverslipped with Entellan (Electron Microscopy Sciences).

In addition, two wild-caught, post-settlement *E. lori* (14, 17 mm SL, 2011) were prepared for paraffin histology. They were decalcified in Cal-Ex for 7–8 h, rinsed in phosphate buffered saline (PBS) for 2 h, dehydrated in ascending series of ethanol and t-butyl alcohol, infiltrated in two changes of Paraplast (Thermo Fisher Scientific) for 4 h (under vacuum), and individually embedded. Blocks were sectioned at a thickness of 8 μm, mounted on slides subbed with 10% albumin in 0.9% NaCl, stained with a modified Hall-Brunt quadruple stain (HBQ; Hall, 1986), and coverslipped with Entellan.

All data from histological material were taken from the right side of each fish (unless the right side was damaged), and bilateral symmetry was assumed. An outline of each fish was drawn to scale (in dorsal, lateral, ventral views) and each neuromast was mapped and assigned a number. The initial and final transverse histological sections in which a neuromast was visible (as defined by thickening of the epithelium and/or presence of hair cells) were recorded. The rostral–caudal length of each neuromast was calculated as the total

**Table 1.** Specimens examined. AMNH or archival (Buston and Webb labs) specimen IDs and methods used to study each specimen. WC = wild-caught; FL = fluorescent vital staining with 4-di-2-ASP; Histology = glycol methacrylate-embedded material, with the exception of two paraffin-embedded fish (par); SEM = scanning electron microscopy. See Materials and Methods for details.

| Species | Specimen ID | # | Size (mm SL) | Age (dph) | FL | Histology | SEM |
|---|---|---|---|---|---|---|---|
| *Elacatinus lori* | | 4 | 3 | 0 | X | | |
| *Elacatinus lori* | | 4 | 4.5 | 10 | X | | |
| *Elacatinus lori* | | 5 | 6–7 | 20 | X | | |
| *Elacatinus lori* | | 5 | 7–9 | 31 | X | | |
| *Elacatinus lori* | | 5 | 8–9.5 | 38 | X | | |
| *Elacatinus lori* | EL G4 F | 1 | 42 | WC | X | | |
| *Elacatinus lori* | EL G12 F | 1 | 44 | WC | X | | |
| *Elacatinus lori* | EL G1 F | 1 | 44 | WC | X | | |
| *Elacatinus lori* | EL G4 M | 1 | 62 | WC | X | | |
| *Elacatinus lori* | EL 101 | 1 | 3 | 0 | | X | |
| *Elacatinus lori* | EL 003 | 1 | 3 | 1 | | X | |
| *Elacatinus lori* | EL 004 | 1 | 3.5 | 2 | | X | |
| *Elacatinus lori* | EL 005 | 1 | 4 | 3 | | X | |
| *Elacatinus lori* | EL 006 | 1 | 4 | 4 | | X | |
| *Elacatinus lori* | EL 007 | 1 | 4 | 5 | | X | |
| *Elacatinus lori* | EL 008 | 1 | 4 | 6 | | X | |
| *Elacatinus lori* | EL 009 | 1 | 4.5 | 7 | | X | |
| *Elacatinus lori* | EL 010 | 1 | 4 | 8 | | X | |
| *Elacatinus lori* | EL 012 | 1 | 4 | 9 | | X | |
| *Elacatinus lori* | EL 015 | 1 | 5 | 10 | | X | |
| *Elacatinus lori* | EL 029 | 1 | 6 | 15 | | X | |
| *Elacatinus lori* | EL 131 | 1 | 6 | 20 | | X | |
| *Elacatinus lori* | EL 141 | 1 | 8 | 24 | | X | |
| *Elacatinus lori* | EL 032 | 1 | 9 | 30 | | X | |
| *Elacatinus lori* | EL 033 | 1 | 9.5 | 34 | | X | |
| *Elacatinus lori* | EL 153 | 1 | 11 | 44 | | X | |
| *Elacatinus lori* | EL 041 | 1 | 14 | WC | | X | |
| *Elacatinus lori* | EL 14 | 1 | 14 | WC | | X (par) | |
| *Elacatinus lori* | EL 17 | 1 | 17 | WC | | X (par) | |
| *Elacatinus lori* | EL 99 | 1 | 2.5 | 0 | | | X |
| *Elacatinus lori* | EL 52 | 1 | 3.5 | 10 | | | X |
| *Elacatinus lori* | EL 99 | 1 | 6.0 | 20 | | | X |
| *Elacatinus lori* | EL 99 | 1 | 8.0 | 27 | | | X |
| *Elacatinus lori* | EL 99 | 1 | 8.0 | 30 | | | X |
| *Elacatinus lori* | EL 99 | 1 | 9.5 | 34 | | | X |
| *Elacatinus lori* | EL 99 | 1 | 11.0 | 40 | | | X |
| *Elacatinus lori* | EL 99 | 1 | 11.0 | 45 | | | X |
| *Elacatinus lori* | | 3 | 9.0–9.5 | WC settler | | | X |
| *Elacatinus lori* | EL G10 F | 1 | 38 | WC adult | | | X |
| *Elacatinus lori* | EL G10 M | 1 | 50 | WC adult | | | X |
| *Elacatinus lori* | EL 105 | 1 | 3 | 2 | | | X |
| *Elacatinus lori* | EL 110 | 3 | 3–4 | 4 | | | X |
| *Elacatinus lori* | EL 114 | 2 | 3.4–4 | 6 | | | X |
| *Elacatinus lori* | EL 118 | 1 | 3.5–4 | 8 | | | X |
| *Elacatinus lori* | EL 122 | 2 | 4–5 | 10 | | | X |
| *Elacatinus lori* | EL 126 | 4 | 4–4.5 | 14 | | | X |
| *Elacatinus lori* | EL 128 | 2 | 5 | 16 | | | X |
| *Elacatinus lori* | EL 130 | 2 | 4.5–5 | 18 | | | X |
| *Elacatinus lori* | EL 134 | 1 | 6 | 20 | | | X |
| *Elacatinus lori* | EL 138 | 1 | 5 | 22 | | | X |
| *Elacatinus lori* | EL 140 | 1 | 6 | 24 | | | X |
| *Elacatinus lori* | EL 145 | 2 | 5.5 | 28 | | | X |
| *Elacatinus lori* | EL 149 | 1 | 7 | 30 | | | X |
| *Elacatinus lori* | EL 152 | 2 | 7–8 | 44 | | | X |
| *Elacatinus colini* | EC 6 | 1 | 9 | 60 | | | X |
| *Elacatinus colini* | EC 6 | 1 | 10 | 60 | | | X |
| *Elacatinus colini* | EC 6 | 1 | 10.5 | 70 | | | X |
| *Elacatinus colini* | EC 6 | 1 | 12 | 70 | | | X |
| *Elacatinus colini* | EC 6 | 1 | 13.5 | 70 | | | X |

**Table 1.** Continued.

| Species | Specimen ID | # | Size (mm SL) | Age (dph) | FL | Histology | SEM |
|---|---|---|---|---|---|---|---|
| *Elacatinus horsti* | AMNH 264763 | 1 | 24 | WC | | | X |
| *Elacatinus puncticulatus* | AMNH 73449 | 1 | 17 | WC | | | X |
| *Elacatinus randalli* | AMNH 238786 | 1 | 18 | WC | | | X |
| *Tigrigobius dilepis* | AMNH 250269 | 1 | 14 | WC | | | X |
| *Tigrigobius gemmatus* | AMNH 26076 | 2 | 15–18 | WC | | | X |
| *Tigrigobius inornatus* | AMNH 233779 | 1 | 19 | WC | | | X |
| *Tigrigobius inornatus* | AMNH 256755 | 1 | 22 | WC | | | X |
| *Tigrigobius multifasciatus* | AMNH 23621 | 2 | 19–22 | WC | | | X |
| *Tigrigobius pallens* | AMNH 26071 | 1 | 12 | WC | | | X |
| *Tigrigobius zebrella* | AMNH 248920 | 2 | 18–19 | WC | | | X |

number of serial sections in which a neuromast was present multiplied by section thickness (5 or 8 μm, for plastic or paraffin histology, respectively).

***Scanning electron microscopy.***—Scanning electron microscopy (SEM) was used to reveal neuromast shape, size, hair cell orientation, and to confirm neuromast locations revealed in fluorescent images and histological material. An ontogenetic series of *E. lori* reared in the lab ($n = 32$, 0–45 dph, 2.5 mm NL–11 mm SL) and additional wild-caught post-settlement fishes (*E. colini*, $n = 5$, 9–13.5 mm SL; *E. lori*, $n = 5$, 9–50 mm SL) had been fixed in 10% formalin in 0.1 M PBS. Museum specimens (species of *Elacatinus* and *Tigrigobius*; Table 1) had been fixed in formalin and transferred to 70% ethanol for long-term storage. All fishes were dehydrated in an ascending ethanol series at room temperature, critical point dried out of liquid $CO_2$ (Tousimis Samdri 780A), and mounted on aluminum stubs using adhesive carbon discs and sputter-coated with platinum (15 nm; Leica MED 020). Fish were viewed with a Zeiss NTS Supra 40VP SEM at 3 kV at a working distance of ~10 mm. Neuromast length, width, area, and sensory strip area were measured in captured digital images using ImageJ (Schindelin et al., 2012) and neuromast number and distribution were documented using the terminology in Sanzo (1911).

***MicroCT imaging.***—Two formalin fixed specimens of *E. lori* were imaged on a Bruker SkyScan 1173 at the Museum of Comparative Zoology (Harvard University). Canal presence, absence, and degree of ossification were confirmed by examining 2D cross sections. Image processing and generation of 3-D volume renderings were carried out using OsiriX (v3.6.1 64 bit).

***Statistical analysis.***—Neuromast counts obtained from fluorescent images and histological material were compared using a paired t-test to determine if the two methods produced comparable results. A mixed-effect ANCOVA was used with neuromast type and fish size as independent variables and neuromast size as a dependent variable (JMP Pro 14) to test for variation of size (length and width) in three neuromast subpopulations (canal neuromasts, canal neuromast homologs, superficial neuromasts) of post-settlement juveniles ("settlers") and adults using SEM imaging and analysis. Individual ID was entered as a random effect to account for the lack of independence among neuromast measurements from the same individual.

To compare the superficial neuromast distribution among species of *Elacatinus* and *Tigrigobius*, data were compiled from SEM images and published accounts (Miller, 1972; Hoese and Reader, 2001) for superficial neuromast lines in 12 species of *Elacatinus* and *Tigrigobius* (Table 2). Superficial neuromast lines with more than four missing values (e.g., counts not attainable due to specimen condition, or availability of images) were excluded from further analysis. Fifteen of the 25 superficial neuromast lines on the cheek visible in lateral view (Table 2) that had fewer than 5% of superficial neuromast count values designated as unknowns were used for this analysis.

Multidimensional scaling (MDS) and analysis of similarity (ANISIM; non-parametric tests) were used to test for significant differences in neuromast number among genera (*Elacatinus*, *Tigrigobius*) and microhabitats ("sponge," "coral," "other"). These data were coded as "abundance" with species data as "rows" and unknown values as "missing" and habitat was added as a factor (using PRIMER v.6 software). The missing number algorithm function was used to generate values for the few remaining unknown superficial neuromast counts using predictions based on known values for the species and interspecies comparisons (Table 2). An MDS plot was created using Euclidean distance to reveal clustering of species from different microhabitats with respect to superficial neuromast counts. An ANISIM test was done using microhabitat (sponge vs. coral vs. "other") and genus (*Elacatinus* vs. *Tigrigobius*) to determine if the clustering pattern revealed in the MDS plot was an artifact of taxonomy (genus) or if it was due to microhabitat differences. A similarity percentage test was then done for each superficial neuromast line to determine which ones explain most of the variation observed in superficial neuromast number among species occupying different microhabitats.

## RESULTS

The lateral line system of *Elacatinus lori* is characterized by a reduced cranial lateral line canal system in which portions of only three lateral line canals are present. In addition, *E. lori* has a proliferation of diamond-shaped neuromasts in a transverse pattern on the skin of the head (neuromast lines under the eye radiate away from the orbit; *sensu* Wongrat and Miller, 1991; see Figs. 1B–D, 2C, 3B). A trunk canal is absent; several lines of neuromasts are found in the skin on the anterior half of the trunk and short vertical lines of neuromasts are found at the horizontal septum on each body segment (myomere; the median series) on the posterior half of the trunk (Fig. 2D–F). A few neuromasts are found at the base of the caudal fin, and three lines of neuromasts sit on

**Table 2.** Number of neuromasts in a subset of cranial neuromast lines in species of *Elacatinus* and *Tigrigobius* based on scanning electron microscopy (in lateral view; see Fig. 3 for definition of neuromast line) in species that occupy different microhabitats (sponge, coral, "other"). All lines are superficial neuromasts, with the exception of u, which is composed of canal neuromast homologs. Values in bold were calculated using the missing value command in PRIMER v.6. * Data from Miller (1972).

| | | Neuromast line | | | | | | | | | | | | | | |
|---|---|---|---|---|---|---|---|---|---|---|---|---|---|---|---|---|
| Species | Habitat | s1 | r | c2 | 2 | 3 | 4 | 5 | 6 | 7 | b | ot | oi | os | x2 | u |
| *E. colini* [a] | sponge | 2 | 3 | 4 | 1 | 2 | 2 | 5 | 1 | 1 | 3 | 12 | 3 | 5 | 5 | 4 |
| *E. horsti* [a] | sponge | 2 | 2 | 4 | 2 | 3 | 4 | 10 | 2 | 1 | 4 | 9 | **4.10** | 3 | 4 | 5 |
| *E. lori* 1 [a] | sponge | 3 | 2 | 4 | 2 | 3 | 4 | 6 | **4.98** | 1 | 4 | 14 | 4 | 4 | 4 | 6 |
| *E. lori* 2 | sponge | 1 | 0 | 3 | 3 | 3 | 4 | 9 | 3 | 1 | 4 | 12 | 6 | 6 | 4 | 6 |
| *E. lori* 3 | sponge | 2 | 3 | 3 | 3 | 3 | 2 | 7 | 4 | 1 | 2 | 12 | 4 | 4 | 4 | 6 |
| *E. lori* 4 | sponge | 2 | 3 | 4 | 2 | 3 | 3 | 9 | 3 | 1 | 4 | 12 | 4 | 4 | 4 | 4 |
| *E. lori* 5 | sponge | 3 | **3.57** | 4 | 3 | 4 | 4 | 9 | 3 | 1 | 5 | 13 | 3 | 4 | 4 | 6 |
| *E. lori* 6 | sponge | 2 | 3 | 4 | 2 | 2 | 3 | 8 | 4 | 1 | 5 | 11 | 4 | 4 | 5 | 5 |
| *E. lori* 7 | sponge | 1 | 2 | 4 | 3 | 3 | 4 | 9 | 3 | 1 | 4 | 14 | 5 | 7 | 5 | 6 |
| *E. oceanops* *[,c] | coral | 2 | 2 | 1 | 3 | 4 | 5 | 9 | 4 | 1 | 5 | 9 | 3 | 3 | 5 | 5 |
| *E. randalli* [b] | coral | 3 | **2.44** | 4 | 2 | 3 | 3 | 6 | 3 | 1 | 3 | 7 | 2 | 3 | **0.89** | **5.48** |
| *T. dilepis* [a] | coral | 2 | 2 | 4 | 2 | **2.62** | **3.07** | 6 | 3 | 1 | 2 | 8 | 3 | 3 | 3 | 4 |
| *T. inornatus* [b] | coral | 2 | 3 | 4 | 2 | 3 | 3 | 6 | 3 | 1 | 3 | **10.42** | **4.12** | **5.20** | 5 | 6 |
| *T. limbaughi* [b] | coral | **2.16** | **1.79** | 1 | 3 | 3 | 2 | 6 | 3 | 1 | 4 | 12 | 3 | 6 | 2 | 7 |
| *T. macrodon* *[,a] | coral | **2.00** | **2.29** | 0 | 2 | 2 | 4 | 5 | 3 | 2 | 5 | 12 | 4 | 6 | 4 | 4 |
| *E. puncticulatus* [b] | other | 2 | 3 | 4 | 2 | 3 | 4 | 9 | 3 | 1 | 4 | 13 | 3 | 4 | 3 | 4 |
| *T. gemmatus* [a] | other | 2 | 2 | 3 | 2 | 3 | 4 | 9 | 4 | 1 | 5 | 12 | 3 | 4 | 3 | 3 |
| *T. multifasciatus* [a] | other | 2 | 3 | 4 | 2 | 3 | 3 | 8 | 2 | 1 | 3 | 11 | 2 | 4 | 2 | 3 |

[a] non-cleaner
[b] facultative cleaner
[c] cleaner (as per Huie et al., 2019)

the membranes between the fin rays of the caudal fin (Figs. 2D, G, 4).

***Lateral line canals and canal neuromasts.***—*Elacatinus lori* retains three pored, ossified cranial lateral line canals (supraorbital, post-otic, and a portion of the preopercular canal); the infraorbital and mandibular canals are absent (Fig. 3). Five canal neuromasts are in the supraorbital canal (in the nasal and frontal bones; Figs. 3A, 5A–D), two canal neuromasts are in the preopercular canal (within the preopercular bone), and one canal neuromast is in the post-otic canal (within the post-temporal bone). In a post-settlement juvenile (14 mm SL), the supraorbital, preopercular, and post-otic canals are enclosed, but do not appear to be fully ossified. Ten canal pores are present, and two of them (λ and κ) are located where the left and right supraorbital canals meet in the midline between the large orbits (Figs. 3A, 5C, D). The pores in the supraorbital and post-otic canals were identified as the σ, λ, κ, ω, α, β, and ρ pores (in rostro-caudal sequence), and the three pores in the vertical portion of the preopercular canal were identified as the δ, γ, and ε pores. Interestingly, two preopercular canal pores were not easily visible in SEMs but were clearly visible in all three post-settlement individuals examined histologically, in one cleared and stained specimen, and in one specimen examined using μCT.

***Neuromast distribution on the skin of adult* E. lori.**—Fluorescence imaging of four adult *E. lori* (42–62 mm SL) revealed 128–155 neuromasts on the skin of one side of the head (Figs. 2A–C, 3). Histological analysis of several post-settlement fish (14–17 mm SL) revealed 124–150 neuromasts. A significant difference in neuromast number determined using these two methods was not found (t-test, $P = 0.134$), so all data reported below are based on fluorescent images unless otherwise stated.

Of the nine neuromast series on the skin of gobies identified by Sanzo (1911), only the interorbital series is missing in *E. lori* and the other eight series are present (Fig. 3):

(1) *Preorbital series* (on the "snout," rostral to the eye; red in Fig. 3A, B) is composed of lines r (0–3 neuromasts), s1 (1–3 neuromasts), s2 (1–3 neuromasts), and c2 (3–4 neuromasts).
(2) *Suborbital series* (running below the eye, on the cheek; Fig. 2C, green in 3B) in *E. lori* is composed of lines 1 (1 neuromast), 2 (2–3 neuromasts), 3 (3–4 neuromasts), 4 (2–4 neuromasts), 5 (7–9 neuromasts), 6 (2–3 neuromasts), 7 (1 neuromast), b (2–5 neuromasts), and d (12–14 neuromasts).
(3) *Preoperculo-mandibular series* (running along the ventral surface of the lower jaw and on the horizontal portion of the preopercular bone; Fig. 2C, yellow in 3B, C) is composed of lines e (14–26 neuromasts), f (2–3 neuromasts), and i (19–24 neuromasts). Line i is rostral to the first pore of the preopercular canal, which is located in the preopercular bone.
(4) *Opercular series* (on the opercular bone; Fig. 2C, orange in Fig. 3B) is composed of lines oi (3–6 neuromasts), os (4–6 neuromasts), and ot (12–13 neuromasts).
(5) *Oculoscapular series* (extending from a point caudal to the orbit to the dorsal margin of the pectoral-fin base; Fig. 2C, blue in Fig. 3A, B) is composed of lines x1 (1–4 neuromasts), x2 (4 neuromasts), u (4–6 neuromasts), z (2–4 neuromasts), as1 (3 neuromasts), as2 (3–5 neuro-

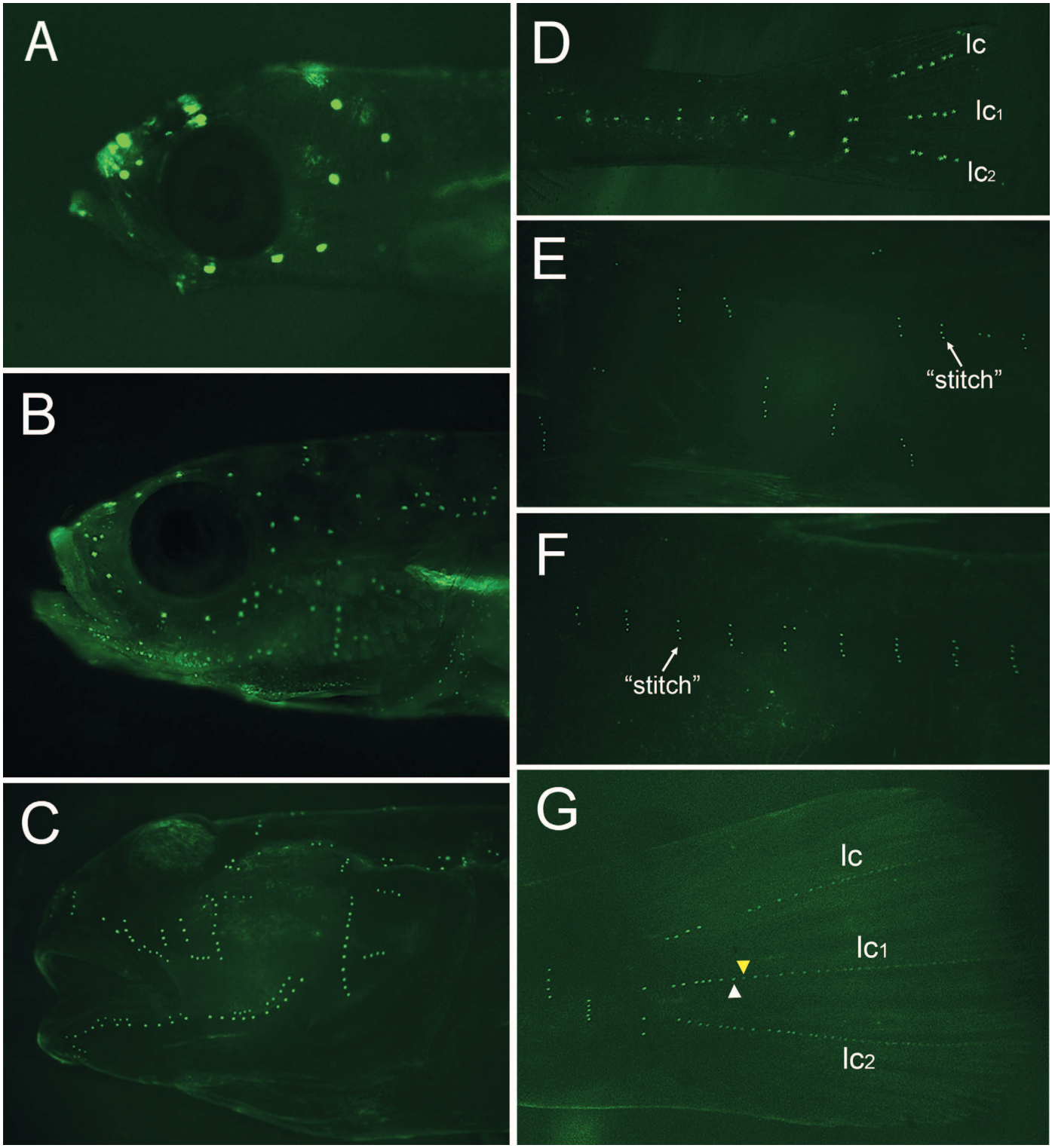


**Fig. 2.** Neuromast distributions in *E. lori* vitally stained with 4-di-2-ASP (lateral view, rostral to the left). (A) 0 dph (3 mm NL; yolk sac larva, fin folds still present) with only nine neuromasts present on head. By 1 dph, the yolk sac is fully absorbed and by 10 dph, flexion has started. (B) 38 dph (9.5 mm SL, pre-settlement) individual with all neuromast lines present on head; only the neuromasts in lines on operculum and mandible have begun to proliferate. Canal neuromasts are still visible (e.g., dorsal to orbit), indicating that the canals are not yet fully ossified. Settlement occurs at ~30–45 dph, 9–11 mm SL. (C) Wild-caught adult (42 mm SL) with lines of proliferated superficial neuromasts on head. (D) Trunk and tail of 20 dph (6 mm SL) larva. The few neuromasts on trunk will proliferate to become short vertical series of superficial neuromasts (see F). A few neuromasts on the caudal fin occur in three lines. (E) Anterior portion of the trunk (adult, 42 mm SL) illustrating several short lines of neuromasts. (F) Posterior portion of the trunk (adult, 42 mm SL) with well-organized vertical lines of neuromasts ("stitches") on each myomere along horizontal septum. (G) Caudal fin (adult, 42 mm SL) with three lines (lines lc, lc1, and lc2) of densely placed neuromasts extending from the fin base to the tip of the caudal fin on the membranes between fin rays. Caudal-fin membranes are so thin that the neuromasts from both the left (white arrowhead) and right (yellow arrowhead) side are visible within a line. See Figures 3 and 4 for identification of neuromast lines.

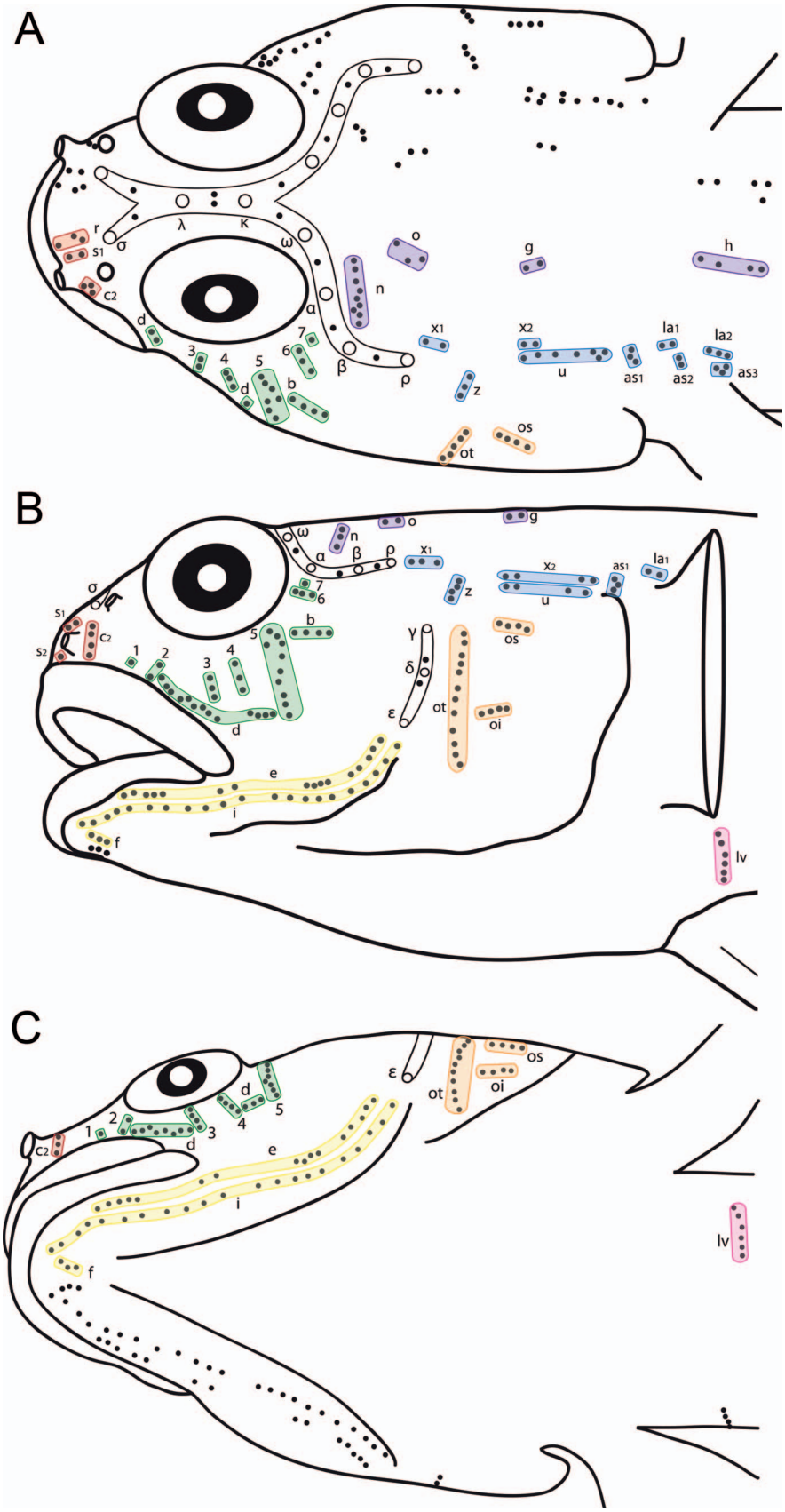


**Fig. 3.** Diagrammatic representation of cranial canals (solid black lines with open pores) and neuromasts (black circles) in *E. lori* based on fluorescent images (see Figure 2) of an adult female (44 mm SL). (A) Dorsal, (B) lateral, and (C) ventral views. A total of 7 series of superficial neuromasts (as defined by Sanzo, 1911) are color coded: red = preorbital, green = suborbital, yellow = preoperculo-mandibular, orange = opercular, blue = oculoscapular, purple = anterior dorsal, and pink = body. The body and caudal series are illustrated in Figure 4. Neuromast lines within series (labeled) are named following Sanzo (1911) and Wongrat and Miller (1991). Position of canals and canal pores based on histological material and labeled following Sanzo (1911).

masts), as3 (3–4 neuromasts), la1 (1–2 neuromasts), and la2 (0–2 neuromasts). Neuromasts rostral to the edge of the operculum are classified as head (cranial) neuromasts and those caudal to the edge of the operculum are classified as trunk neuromasts. In this series, lines as1–3 and la1–2 are considered trunk neuromast lines while all the rest are considered to be head (cranial) neuromast lines.

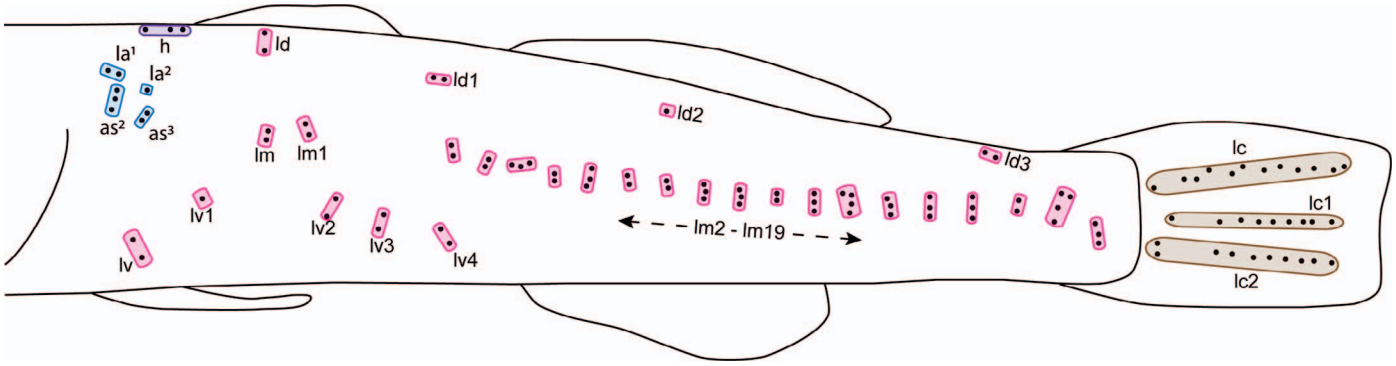


**Fig. 4.** Distribution of superficial neuromasts (black circles) in body and caudal series in an *E. lori* post-settlement juvenile ("settler"; 38 dph, 9.5 mm SL) based on fluorescent images (see also Fig. 2D–G). Superficial neuromast series (defined by Sanzo, 1911) are color-coded: blue = oculoscapular, purple = anterior dorsal, pink = body, and brown = caudal. Names for superficial neuromast lines within series follow Sanzo (1911) and Wongrat and Miller (1991). The large pectoral fin is not drawn in order to visualize all neuromasts on the trunk. See text for additional details.

(6) *Anterior dorsal series* (extending caudally from the eye to the anterior insertion of the dorsal fin; purple in Fig. 3A) is composed of lines g (2–3 neuromasts), h (1–5 neuromasts), n (3–10 neuromasts), and o (3–4 neuromasts).

(7) *Interorbital series* (region between eyes) is absent in *E. lori*.

(8) *Body series* (on the trunk; Fig. 2D–G, pink in Fig. 4) is composed of three groups of lines: dorsal, median, and ventral. Three short vertical lines (dorsal lines) are located just ventral to the first dorsal fin: ld (5–6 neuromasts), ld1 (2–3 neuromasts), and ld2 (2–3 neuromasts). An enclosed trunk canal is absent, but a short superficial neuromast line (or stitch) sits over each myomere where a lateral line scale containing a canal segment would typically be found in other fishes. A total of 19–22 vertical lines (median lines lm to lm21) each comprised of three to five neuromasts are found along the horizontal septum (mid-flank), for a total of 65–80 neuromasts on the skin of the trunk. In addition, five or six short, vertical lines are located caudal to the pectoral fin on the lower third of the body (ventral lines): lv (6–14 neuromasts, obscured by pectoral fin), lv1 (2–5 neuromasts), lv2 (5–8 neuromasts), lv3 (5–6 neuromasts), lv4 (5–8 neuromasts), and lv5 (0–2 neuromasts). All three groups of lines (dorsal, median, ventral) are found on the anterior portion of the trunk (obscured by the pectoral fin when in resting position), while only the highly organized vertical lines of the median series are found on the trunk caudal to the pectoral fin.

(9) *Caudal series* (on the caudal fin; Fig. 2D, G, brown in Fig. 4) is composed of a short vertical line of four neuromasts at the base of the caudal fin and three lines that sit on the membranes between caudal-fin rays and extend caudally, to the tip of the caudal fin. In the short vertical line of neuromasts at the base of the fin the bottom two form part of line lc2. The three long lines of closely placed neuromasts (~100 μm apart) on the caudal fin are aligned side-by-side: lc (9–16 neuromasts), lc1 (6–16 superficial neuromasts), and lc2 (12–26 neuromasts). Line lc1 is located in the midline of the caudal fin. Lines lc and lc2 are located in the membranes between fin rays dorsal and ventral to lc1, but not those directly adjacent to lc1. Neuromasts on both sides of the caudal fin are visible in fluorescent images because the fin membranes are translucent (Fig. 2G). This likely accounted for the variability in the number of neuromasts observed among specimens.

***Neuromast morphology and their arrangement within lines.***— All neuromasts in *E. lori* are relatively small (~40 μm long) in post-metamorphic juveniles and adults, and they are diamond-shaped (length = ~2x width) with a central, oval sensory strip (Figs. 5I, J, 6A, 7). In all neuromasts, the long axis of the oval defining the sensory strip and the axis of best physiological sensitivity of the hair cells (as determined by kinocilium placement relative to the stereocilia in each hair cell) are both perpendicular to the long axis of the neuromast (Fig. 6A, B). As in other gobies, the neuromasts occur in lines within the cranial canals and on the skin of the head, trunk, and caudal fin. Neuromasts *within* a line are all arranged in the same way, but two different neuromast arrangements ("tip-to-tip," "side-by-side") are found *among* lines (Figs. 7, 8). Most of the superficial neuromasts on the head and the neuromasts on the trunk are aligned tip-to-tip, with the long axis of all of the neuromasts *parallel* to the line in which they are found. In these lines, the long axis of the oval sensory strip and hair cell orientation are perpendicular to the long axis of the neuromast and thus to the line of neuromasts (Fig. 6A, B, 7, 8C). In contrast, the canal neuromasts on the head and the superficial neuromasts on the caudal fin are aligned side-by-side, with the long axis of the neuromasts *perpendicular* to the line in which they are found (Figs. 7F, 8A, B). A small number of neuromasts on the head are also arranged side-by-side and are thus distinct from the other superficial neuromasts on the head (Fig. 8B). Based on their arrangement within lines and their location, often at the ends of short cranial canals (e.g., lines i and u; Figs. 3B, 7C), it is hypothesized that they are canal neuromast homologs ("replacement neuromasts," *sensu* Coombs et al., 1988), canal neuromasts that are now located on the skin, but had been enclosed in ancestral canals, which are absent.

Neuromasts in all three sub-populations (canal neuromasts, canal neuromast homologs, and superficial neuromasts) are small and diamond-shaped, with some variation in neuromast length and/or width (e.g., robust vs. slender diamonds; Fig. 9) in post-settlement juveniles (settlers) and adults. A mixed model analysis revealed that neuromast length (Fig. 9A) varies with fish size (df = 1, f-ratio = 60.2436,

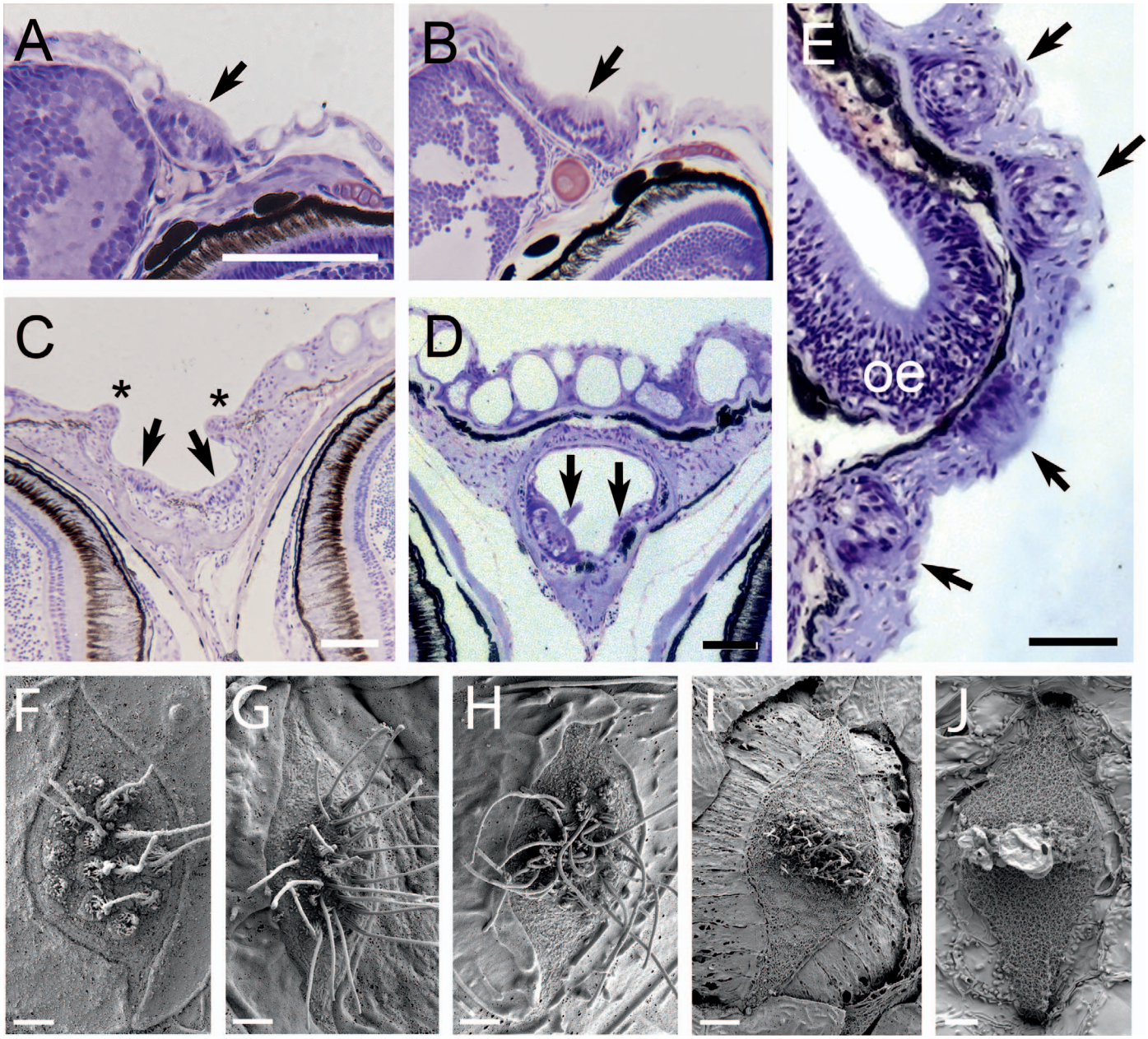


**Fig. 5.** Lateral line development in *E. lori*. (A–E) Supraorbital (SO) canal with canal neuromasts (CNs) between orbits and superficial neuromasts in larvae. (A) CN (arrow) prior to canal enclosure (Stage I) at 0 dph. (B) CN (arrow) in depression as canal formation starts (Stage IIa) at 10 dph (5 mm SL). Nuclei of cells in two layers are visible in the neuromast (upper layer, sensory hair cells; lower layer, non-sensory support cells). (C) Left and right CNs (arrows) in the SO canal in the dorsal midline, with canal walls rising (*, Stage IIb), but not yet enclosing the CNs. (D) Left and right CNs (arrows, as in C; cupula of left neuromast is visible) are enclosed in the ossified SO canal (Stage IV; wild-caught settler, 14 mm SL). (E) Example of a line of densely placed superficial neuromasts (line c2) in wild-caught settler (14 mm SL) in the nasal area; prominent olfactory epithelium (oe). Stages of canal development (I–IV) follow Webb and Shirey (2003). (F–J) Ontogeny of superficial neuromast size and shape in *E. lori* showing diamond shape and gradual restriction of hair cells to a central, oval sensory strip. Axis of best physiological sensitivity (hair cell orientation) is perpendicular to the long axis of the neuromast. (F) 0 dph—neuromast on trunk is already diamond-shaped, (G) 10 dph—neuromast on trunk, (H) 20 dph—neuromast on cheek, (I) 34 dph—neuromast on cheek, note that sensory strip takes up a smaller portion of area of the neuromast compared to those in F–H. (J) Adult—superficial neuromast on caudal fin. Scale bars: A–E, 50 μm; F–H, 2 μm; I–J, 5 μm.

$P = 0.006$) and neuromast type (subpopulation; df = 4, f-ratio = 5.0789, $P = 0.0002$). *Post hoc* tests revealed that canal neuromast homologs on the head are significantly longer than superficial neuromasts on the trunk (Tukey's HSD: $P < 0.05$), and superficial neuromasts on the head are significantly longer than superficial neuromasts on the trunk (Tukey's HSD: $P < 0.05$). All other comparisons of neuromast length between neuromasts of different types and locations (head, trunk, tail) were not significant. The whole model explained an estimated 81.01% of the variation in neuromast length. A second mixed model revealed that neuromast width (Fig. 9B) varies with fish size (df = 1, f-ratio = 6.0849, $P = 0.0175$) and neuromast type (subpopulation; df = 4, f-ratio = 26.2121, $P < 0.0001$). *Post hoc* tests indicated that head canal neuromasts and head canal neuromast homologs are significantly wider than both superficial neuromasts on the

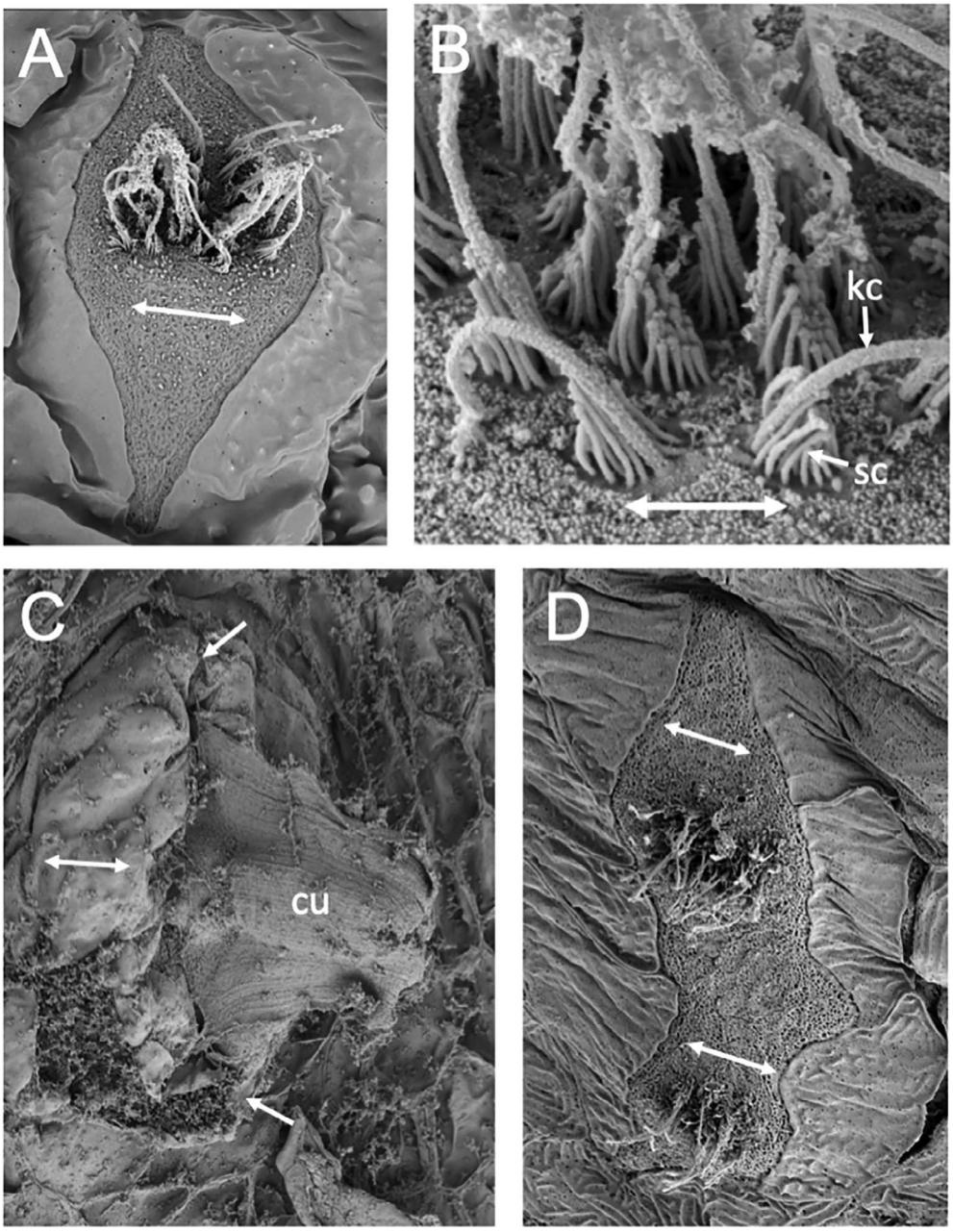


**Fig. 6.** Neuromast and cupular morphology in *E. lori*. (A) Neuromast showing hair cells in central sensory strip with opposing polarities (hair cell orientation; double-headed arrow). (B) Detail of neuromast, as in A, showing ciliary bundles of individual hair cells (each with kinocilium [kc] and multiple stereocilia [sc]) with opposing polarities. (C) Gelatinous cupula (cu) retained on a neuromast that has the same orientation as neuromast in A; note the "wing-like" extensions of the cupula that reaches to the tips (arrows) of the elongate neuromast. (D) Neuromast that appears to be in the process of budding, which is thought to be the mechanism for neuromast proliferation. Double-headed arrows = hair cell orientation.

head and superficial neuromasts on the trunk and tail (Tukey's HSD: $P < 0.05$). Furthermore, superficial neuromasts on the head are significantly wider than those on the trunk and tail (Tukey's HSD: $P < 0.05$). All other comparisons of neuromast width between neuromasts of different types and locations (head, trunk, tail) were not significant. The whole model explained an estimated 80.75% of the variation in neuromast width.

To summarize, on the head, canal neuromasts are wider, but not longer, than superficial neuromasts. Canal neuromast homologs are also wider than superficial neuromasts on the head, but they are neither longer nor wider than the canal neuromasts. Canal neuromast homologs are, however, longer and wider than superficial neuromasts on the trunk and they are wider than the superficial neuromasts on the tail. The superficial neuromasts on the head are longer and wider than the superficial neuromasts on the trunk, and wider than the superficial neuromasts on the tail. The superficial neuromasts on the trunk and tail are not significantly different with reference to either length or width.

***Ontogeny of superficial neuromast proliferation in* E. lori.**—The process of neuromast proliferation in *E. lori* appears to occur in a relatively simple manner (Fig. 6D). At hatch, larvae have 22 neuromasts, which are found in only six of the eight neuromast series (each comprised of only a few of the superficial neuromast lines found in adults; Fig. 10A). On the head, two supraorbital and one preopercular presumptive canal neuromasts and eight superficial neuromasts are present. Of the 33 neuromast lines on the head in adults, only eight are present at hatch, with one neuromast in each (in lines r, c2, 5, b, i, u, n, and h). In addition, most of the neuromasts are already diamond-shaped and they continue to increase in size throughout ontogeny. The number of canal neuromasts present increases from three at eight days

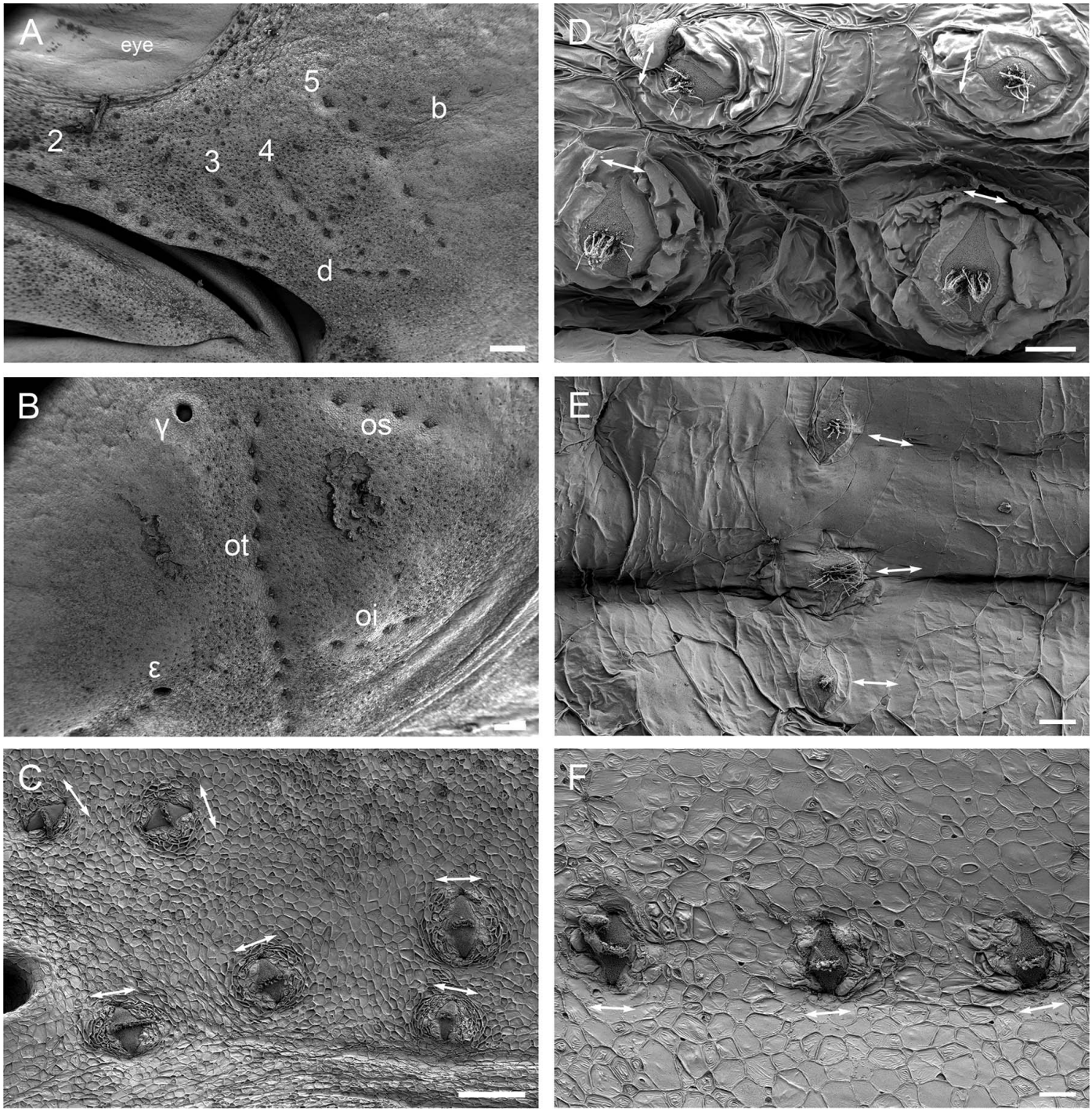


**Fig. 7.** Superficial neuromasts and canal neuromast homologs on the head and trunk in *E. lori* (rostral to left in all images). (A) Radiating lines of superficial neuromasts (lines 2, 3, 4, 5, b, and d) on cheek (lateral view). (B) Superficial neuromast series (lines ot, os, and oi) form an "F" on operculum (lateral view); preopercular canal pores (ε, γ) visible. (C) Post-otic region of head (caudal to post-otic canal pore); upper pair of SNs are aligned tip-to-tip and lower group of neuromasts extending caudally from the canal pore are aligned side-by-side (interpreted as canal neuromast homologs). (D) Portion of the double line of neuromasts on mandible (in ventral view), in which the neuromasts in the upper (more lateral) line have a tip-to-tip arrangement (line e; superficial neuromasts) and those in the lower (more median) line have a side-to-side arrangement (line i; canal neuromast homologs). (E) On the trunk, a line of three superficial neuromasts at the horizontal septum arranged tip-to-tip. (F) Middle row of superficial neuromasts on caudal fin (line lc1) aligned side-to-side. Double-headed arrows indicate axis of best physiological activity of hair cells in all images. Scale bars: A–B, 200 μm; C, 100 μm; D–E, 10 μm; F, 20 μm.

post-hatch (dph) to eight at 15 dph (~5 mm SL; Figs. 10, 11) and then remains constant throughout life. The cranial canal neuromasts become enclosed in canals around settlement (~30–45 dph). The number of superficial neuromasts on the head increases linearly with size ($r^2 = 0.98$; Fig. 11), and the number of lines and the number of superficial neuromasts within each line also increases. All six series on the head, comprised of 33 neuromast lines, are present at 30–40 dph

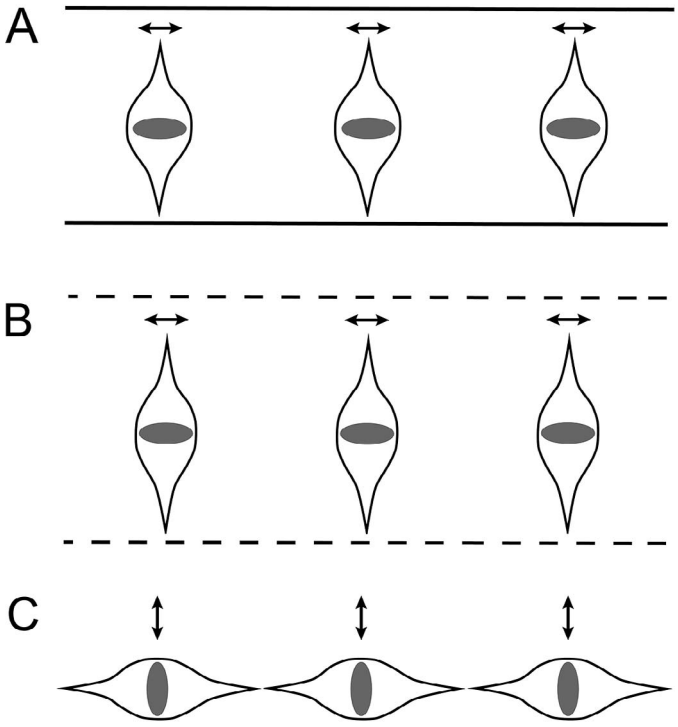


**Fig. 8.** Neuromast arrangements within lines in *E. lori* and other goby species examined. (A) Canal neuromasts, aligned "side-by-side" with axis of best physiological sensitivity parallel to the length of the canal and line of neuromasts (black lines represent canal walls). (B) Canal neuromast homologs or caudal fin superficial neuromasts, arranged "side-by-side" with axis of best physiological sensitivity parallel to line of neuromasts. On the caudal fin, each neuromast line is located on the membrane between adjacent fin rays. Dashed lines represent location of canal walls (in an ancestral canal) on the head or the fin rays on the tail. (C) Superficial neuromasts aligned "tip-to-tip" with axis of best physiological sensitivity perpendicular to line. Gray area = sensory strip. Double-headed arrow = axis of best physiological sensitivity (hair cell orientation).

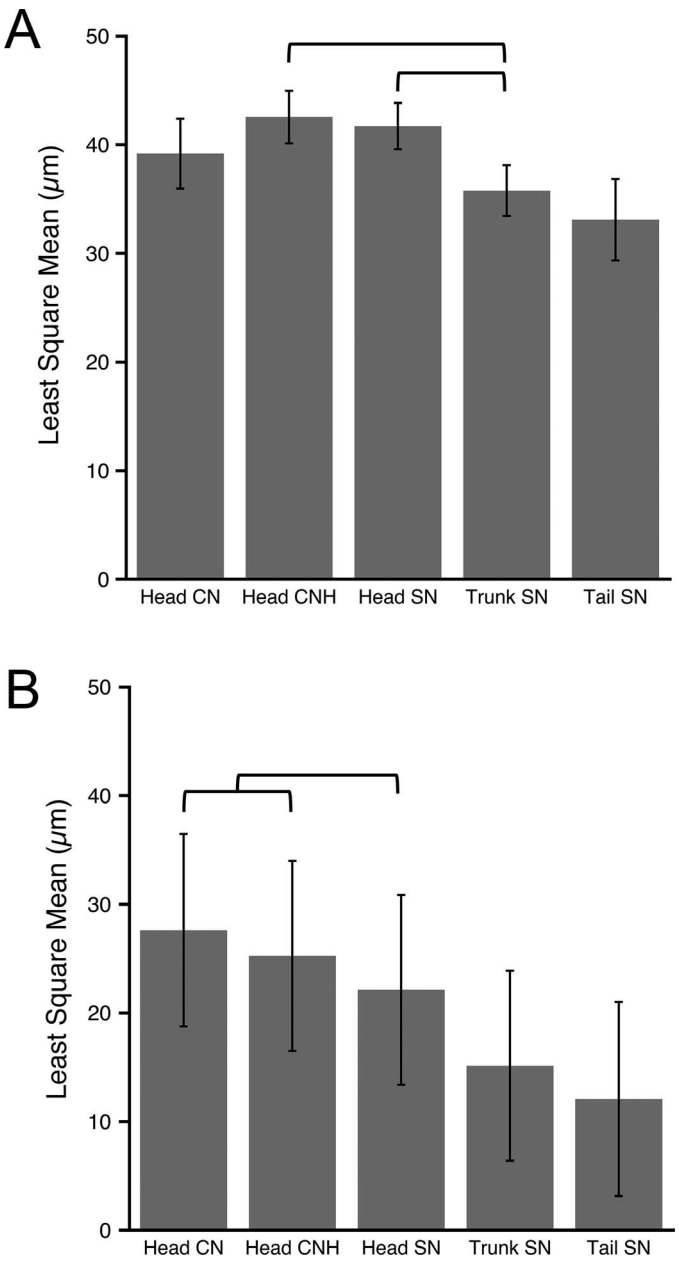


**Fig. 9.** Comparison of neuromast size in post-settlement juveniles and adult *E. lori*. Least squared means of (A) neuromast length and (B) neuromast width and standard error are plotted for each neuromast type (canal neuromasts [CN], canal neuromast homologs [CNH], superficial neuromasts [SN])—Head CN ($n = 13$), Head CNH ($n = 45$), Head SN ($n = 102$), Trunk SN ($n = 65$), and Tail SN ($n = 8$)—based on linear measurements of scanning electron micrographs. Statistically significant differences are indicated by brackets (*post hoc* Tukey's HSD, $P < 0.05$).

(~7–10 mm SL). Neuromast lines in the oculoscapular series (see Fig. 3) are the last to appear. As a result of this developmental process, adults have a total of 307–332 neuromasts (canal neuromasts, canal neuromast homologs, and superficial neuromasts).

On the trunk, neuromast number increases from 10 to 30, with one ultimately positioned over each myomere (Figs. 2F, 4, 10). At 20 dph, the neuromasts on each myomere form vertical lines (aligned tip-to-tip, with rostro-caudal hair cell orientation), each comprised of 2–5 neuromasts (Figs. 2D, F, 4, 10D, E). On the caudal fin, neuromasts are not apparent at hatch (0 dph; Fig. 10A), but at least three neuromasts are present in each of three caudal-fin lines at 20 dph (Figs. 2D, 10C). The number in each line then increases so that each is composed of 6–26 neuromasts in settlers and adults (Figs. 2G, 4, 10E).

***Lateral line system in species of* Elacatinus *and* Tigrigobius *from different microhabitats.*—**In addition to *E. lori*, four other species of *Elacatinus* and six species of *Tigrigobius* (Tables 1, 2) were examined using SEM to determine the number, distribution, and shape of neuromasts on the skin. All species examined have a transverse neuromast configuration with neuromast lines (lines 1–7) radiating from the lower margin of the orbit (Figs. 1C, 2C, 12A; Wongrat and Miller, 1991). The overall pattern and distribution of neuromasts was similar among species; the eight series of neuromasts in *E. lori* are found in all species examined. The double line of the preopercular-mandibular series (lines e and i; Fig. 3C) and the opercular series (lines ot, oi, and os; which form the "F" configuration on the cheek; see Figs. 1, 2C, 3B, 7B) were observed in all species in which the cheek was in good condition (Fig. 12; e.g., data not available for *E. horsti* and *T.*

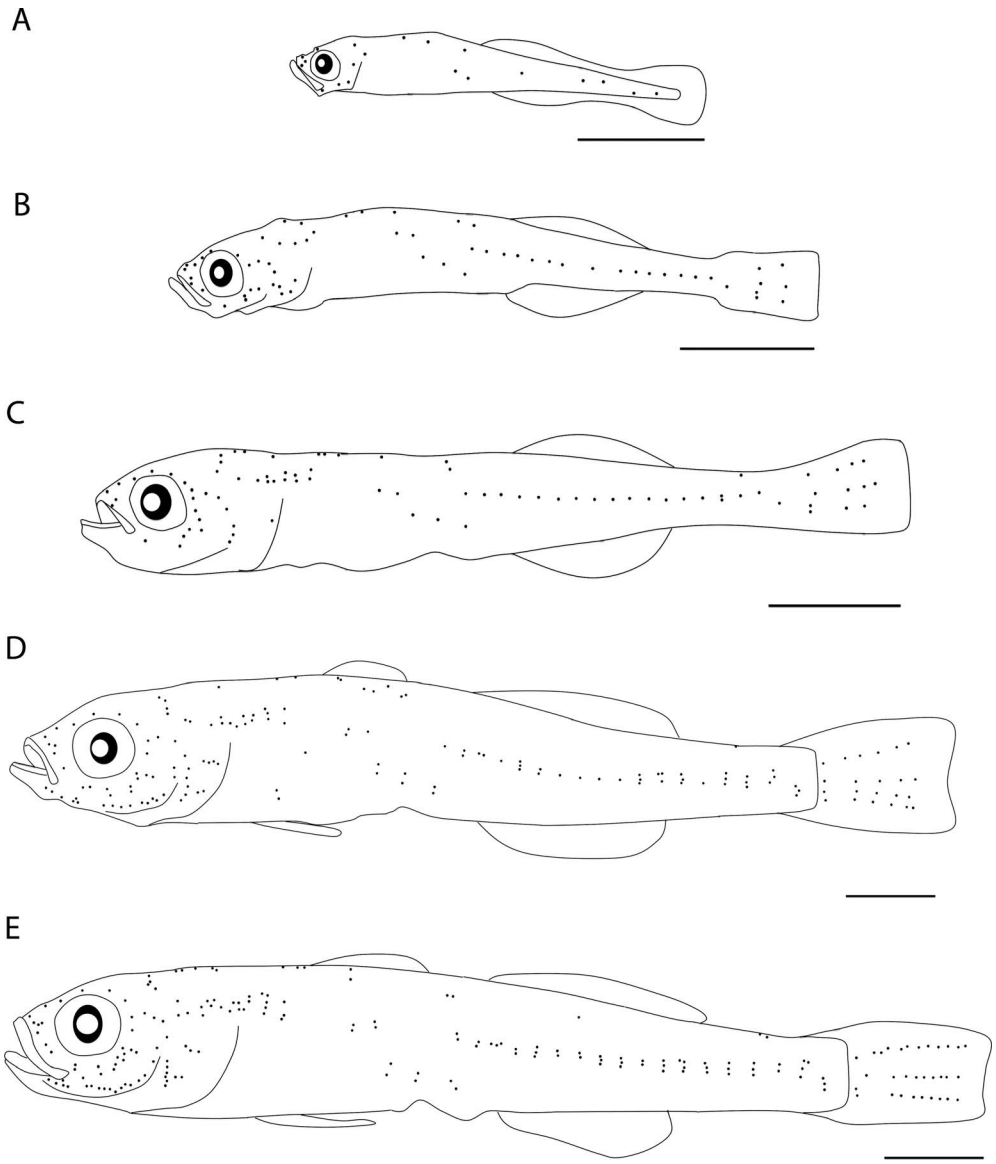


**Fig. 10.** Ontogeny of neuromast distribution in *E. lori* derived from fluorescent images. (A) 0 dph, 3 mm TL; (B) 10 dph, 4.5 mm SL; (C) 20 dph, 6.5 mm SL; (D) 31 dph, 9 mm SL; and (E) 38 dph, 9 mm SL presettlement larva. Pectoral fin removed to facilitate visualization of all neuromasts on the trunk. Yolk sac not drawn. Scale bar = 1 mm. See Figures 3 and 4 for identity of neuromasts.

*zebrella*). In all species, neuromasts appear to be located on papillae that vary in length among species.

As in *E. lori*, the other species examined have elongate diamond-shaped neuromasts with an oval central sensory strip in which hair cell orientation is perpendicular to the long axis of the neuromast (Fig. 12E, F). Within most lines, neuromasts are aligned tip-to-tip with the long axis of the neuromast parallel to the line and hair cell orientation (axis of best physiological sensitivity) perpendicular to the line (Fig. 12C–F). The neuromasts in other lines are aligned side-by-side with the axis of best physiological sensitivity of hair cells parallel to the neuromast line and thus to the axis of the ancestral canal; these are hypothesized to be canal neuromast homologs.

SEM analysis revealed that all species of *Elacatinus* and *Tigrigobius* examined have a supraorbital canal with at least four pores and a preopercular canal with at least two pores (Fig. 12C). It is likely that all species have five supraorbital canal pores, but not all of the pores could be visualized due to specimen condition and the limited number of images obtained in *T. inornatus* and *T. zebrella*.

Neuromast counts in a subset of neuromast lines on the skin on the head were successfully obtained from SEM images (Table 2). A statistical comparison of neuromast number with respect to microhabitat among all species (including *E. lori*; analysis of similarity; Fig. 13) showed that microhabitat (sponge, coral, or "other") had a significant effect on superficial neuromast number ($P = 0.026$), while genus (*Elacatinus* vs. *Tigrigobius*) had no significant effect ($P = 0.25$). Sponge-dwelling species have more neuromasts when compared to coral-dwelling species ($P = 0.004$), but no differences were found when comparing species from sponge vs. "other" or coral vs. "other" microhabitats ($P = 0.532$ and $P = 0.381$, respectively). It should be noted that most of the sponge-dwelling species examined are in *Elacatinus*, and most of the coral-dwelling species are in *Tigrigobius*, but genus did not have a significant effect on neuromast number ($P = 0.25$). The greatest difference in neuromast number was found in species occupying sponge versus coral microhabitats and further, this difference was primarily attributed to differences in neuromast number in five lines (ot, 5, c2, x2, and os) representing 71.22% of the differences observed

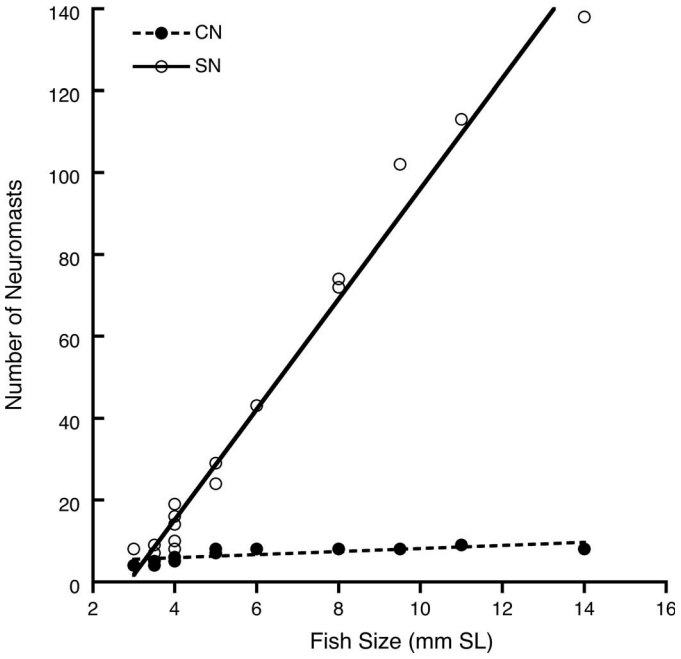


**Fig. 11.** Ontogeny of neuromast number on one side of head in *E. lori* larvae and post-settlement juveniles (0–44 dph and wild-caught settler) based on histological material. Black circles = canal neuromasts, open circles = canal neuromast homologs + superficial neuromasts. Canal neuromast number increases to a constant ($n = 8$), which is reached at ~6 mm SL (~15 dph), while canal neuromast homologs and superficial neuromast number increase in number with fish size ($R^2 = 0.982$).

between sponge- and coral-dwelling taxa (similarity percentage test).

## DISCUSSION

The mechanosensory lateral line system of *Elacatinus lori* was described in detail for the first time and three subpopulations of neuromasts are defined. The description of the post-embryonic ontogeny of the lateral line system (from hatch through settlement) is the first for any gobiiform species. The functional implications of neuromast morphology and neuromast arrangement within lines and the pattern of development are considered. Further, the comparison of neuromast numbers among species of *Elacatinus* and species in its sister genus, *Tigrigobius*, suggests some functional and ecological correlates.

***Neuromast morphology.***—All of the neuromasts in *E. lori* and the other species examined are diamond-shaped regardless of subpopulation (canal neuromasts, canal neuromast homologs, superficial neuromasts) or location on head, trunk or tail. Diamond-shaped neuromasts have been reported in 4 of 12 groups within the Gobiidae (defined by Thacker and Roje, 2011): American seven-spined gobies (*Elacatinus* spp., *Tigrigobius* spp., this study; *Gobiosoma ginsburgi*, unpubl. data), Ponto-Caspian and Mediterranean gobies (*Gobius niger*, Marshall, 1986; *Neogobius melanostomus*, unpubl. data), crested gobies (e.g., *Coryphopterus glaucofraenum*, unpubl. data), and inshore gobies (*Bathygobius fuscus*, Rouse and Pickles, 1991a). Diamond-shaped neuromasts are also known in representatives of other gobioid families (as defined in Thacker, 2009): *Rhinogobius* sp. (Gobionellidae, Watanabe et al., 2010) and *Gobiomorphus cotidianus* (Eleotridae, Bassett et al., 2006). Thus, diamond-shaped neuromasts may have evolved independently several times within the Gobiidae and other gobioid families, or they may represent a conserved feature uniting one or more larger groups within the Gobioidei or within the Gobiiformes.

The neuromasts in *E. lori* are also interesting for several other reasons. They are all small (mean length <50 μm) and diamond-shaped (as noted in another goby; *Gobius niger*, Marshall, 1986), but some significant variation was found in neuromast size and shape (length vs. width) among subpopulations of neuromasts on the head, trunk, and tail (Fig. 9). This is in contrast to the morphology in a range of taxa in which canal neuromasts are notably larger than superficial neuromasts and are often distinct in shape (with no distinction between canal neuromast homologs and superficial neuromasts, as defined here; e.g., Janssen et al., 1987; Münz, 1989; Puzdrowski, 1989; Song and Northcutt, 1989; Faucher et al., 2003; Becker et al., 2016; reviewed in Webb, 2014a). Second, neuromasts in *E. lori* increase in size (e.g., length increases from ~30 μm in larvae to 45 μm in *E. lori* settlers and 50–85 μm in adults), but neuromasts in larvae are already diamond-shaped. The larvae of other fishes typically have round neuromasts that change shape as transformation approaches (zebrafish, Webb and Shirey, 2003; barramundi, Mukai et al., 2007; cichlids, Becker et al., 2016; brown-marbled grouper, Mukai and Lim, 2016).

***Neuromast arrangements within lines.***—The neuromasts in *E. lori* belong to three subpopulations defined by their location in canals, their proximity to existing canals, their location with respect to ancestral canals (which are absent), or the absence of an association with canals. The evolution of the reduced canal pattern in gobiids (and in other taxa) presumably occurred via a simple truncation of the process of canal morphogenesis (Webb, 2014b). Whereas *Rhyacichthys aspro* (a member of Rhyacichthyidae, a basal gobioid family, Thacker, 2009; Thacker et al., 2015), retains a well-developed set of lateral line canals on the head and trunk (Asaoka et al., 2014), *E. lori* retains only three cranial canals (supraorbital, preopercular, post-otic). The neuromasts within the canals in *E. lori* are diamond-shaped and arranged side-by-side with the long axis of the neuromast perpendicular to the canal axis, but hair cell orientation is parallel to the canal axis (Fig. 9A), thus ensuring their ability to respond to water movement along the length of the canal.

The evolutionary reduction of the lateral line canals in gobies resulted in canal neuromasts remaining on the skin. The current study has shown that in *E. lori* these canal neuromast homologs (the ancestral otic, post-otic, infraorbital, and mandibular canal neuromasts) are neither longer nor wider than the canal neuromasts in the remaining canals (although they are wider than superficial neuromasts). The canal neuromast homologues retain a side-by-side arrangement with hair cell orientation parallel to the axis of the ancestral canal (Fig. 8A, B). Thus, the morphology and arrangement of the canal neuromast homologs have been conserved despite being released from the spatial and functional constraints associated with enclosure within the lateral line canals. The third subpopulation of neuromasts, the superficial neuromasts, have a tip-to-tip arrangement, such that hair cell orientation is perpendicular to the line in which they are found (Fig. 8C). These lines tend to be oriented with respect to either the body axes (e.g., dorso-

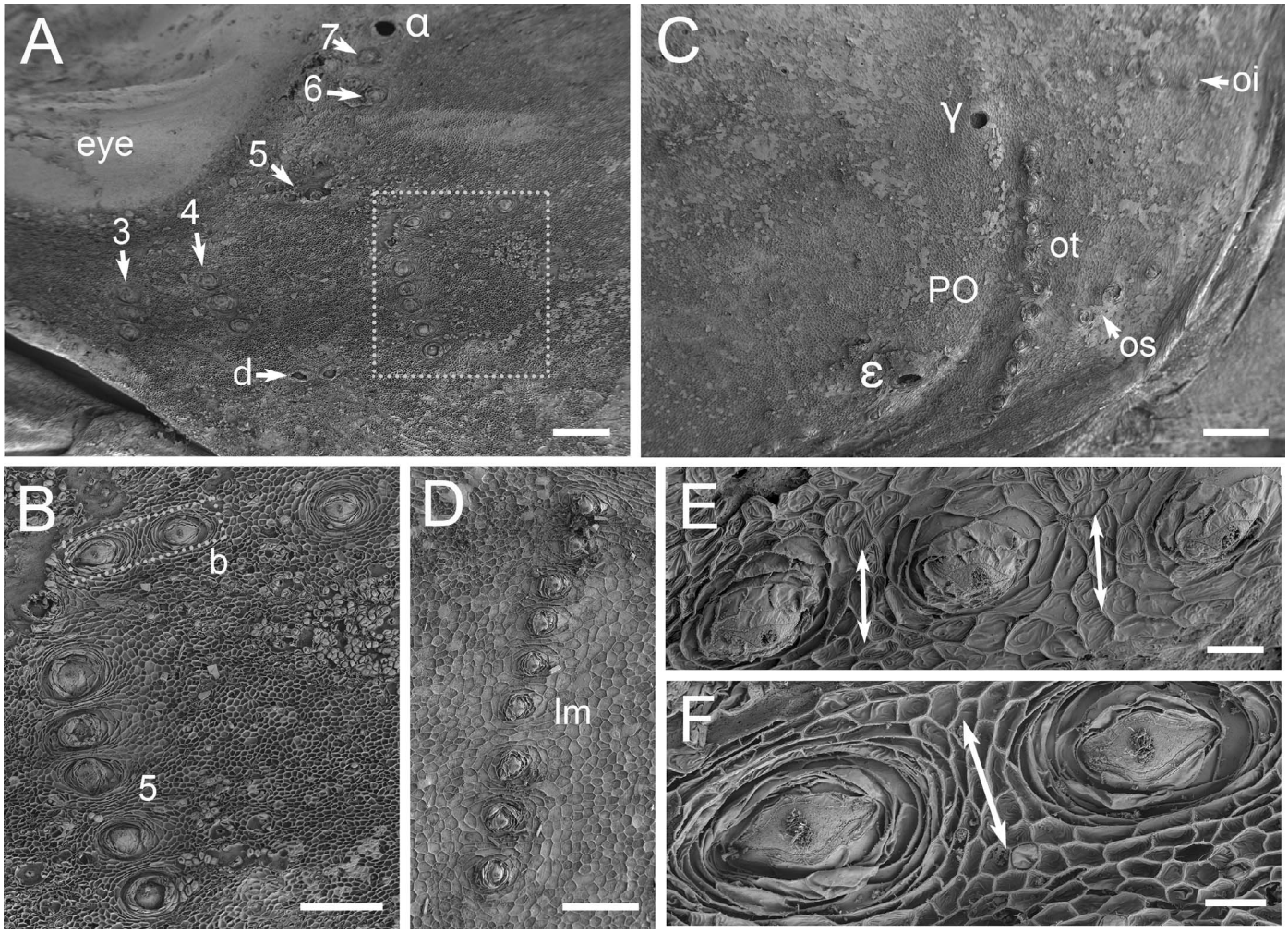


**Fig. 12.** Neuromast morphology in species of *Tigrigobius* (lateral views; rostral to left). (A) *T. multifasciatus* (AMNH 23621)—radiating superficial lines on the cheek (3, 4, 5, b, d; see Fig. 3B). (B) Lines 5 and b (see box in A), which have a tip-to-tip arrangement. (C) *T. gemmatus* (AMNH 26076)—preopercular canal (PO) pores (ε, γ) and opercular series (lines ot, os, oi, forming the "F" on the operculum). (D) *T. gemmatus* (AMNH 26076)—superficial neuromast line on trunk just caudal to tip of pectoral fin when against body. (E) *T. dilepis* (AMNH 250269)—diamond-shaped superficial neuromasts in line os (ventral horizontal line in "F" on operculum) with "tip-to-tip" arrangement and hair cell orientation (double-headed arrows) perpendicular to line. (F) *T. gemmatus* (AMNH 26076)—first two diamond-shaped superficial neuromasts in line b (see box in B) with "tip-to-tip" arrangement and hair cell orientation (double-headed arrows) perpendicular to line. Scale bars: A, C, 200 μm; B, D, 100 μm; E–F, 20 μm.

ventrally, rostro-caudally) or features of the head (e.g., around the orbit). The exception is represented by the superficial neuromasts on the caudal fin, which have a side-by-side arrangement like that of canal neuromast homologs (Fig. 8B).

Superficial neuromasts may be further categorized based on their placement relative to canals or to lines of canal neuromast homologs. For instance, some superficial neuromasts occur independently of any of the canals or lines of canal neuromast homologs (e.g., those that form the "F" on the operculum; Figs. 1A, C, 2C, 3B, 7B). However, others may form an "accessory line" that accompanies a canal or line of canal neuromast homologs. In this situation, their tip-to-tip arrangement provides complementary (orthogonal) directional sensitivity to the canal neuromasts or canal neuromast homologs that they accompany. One example is the double line of neuromasts on the mandible common among the species studied (Figs. 2C, 3B, C, 7D) and other gobiids (*Gobiosoma ginsbergi,* unpubl. data; Takagi, 1957; Marshall, 1986; Ahnelt and Scattolin, 2003) and eleotrids (Bassett et al., 2006). The more lateral of the two lines (line e; Figs. 3C, 7D) is comprised of neuromasts aligned tip-to-tip like other superficial neuromast lines on the head. In contrast, the neuromasts in the more medial line (line i; Fig. 7D) are aligned side-by-side. The neuromasts comprising line e, which demonstrate a tip-to-tip arrangement, are interpreted to be those that accompany the canal neuromast homologs comprising line i (as in Marshall, 1986). This interpretation is also supported by the neuromast configuration in *Rhyacichthys aspro* in which line e is present, but superficial neuromasts of line i are not present and a mandibular canal containing canal neuromast is retained (Asaoka et al., 2014). Similarly, in *E. lori*, line u extends rostro-caudally from the last (most caudal) canal pore (pore ρ) of the short post-otic canal (Fig. 7C), and its neuromasts are likely canal neuromast homologs that had been enclosed in the portion of the post-otic canal in ancestral taxa. The innervation of neuromasts in line u in eleotrids, which is similar to that of the canal neuromasts in species lacking the post-otic canal (Wongrat and Miller, 1991), supports this interpretation. These dis-

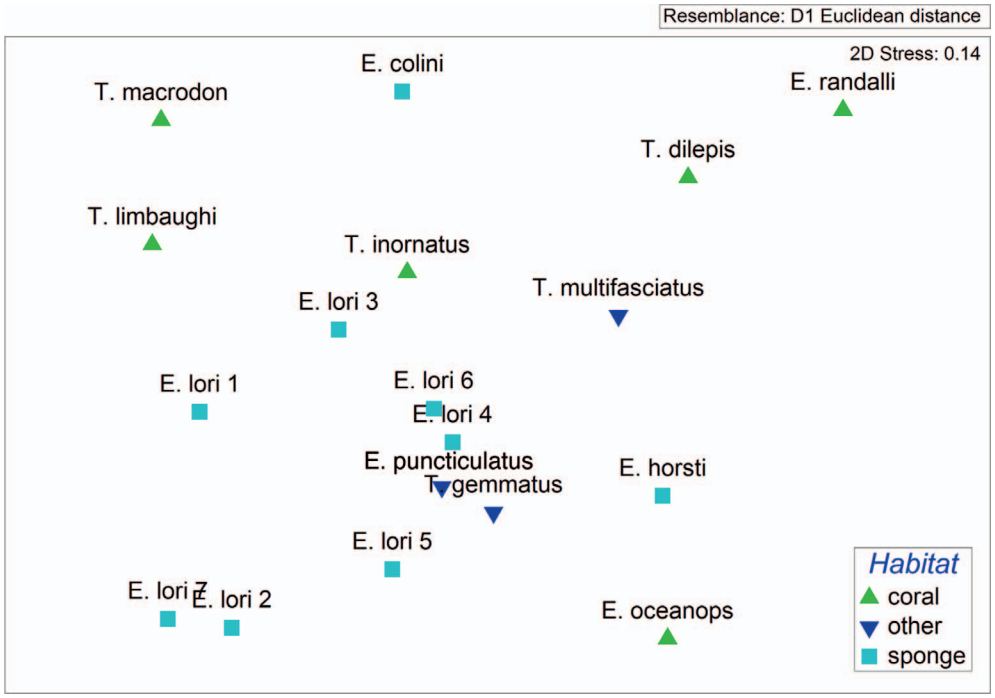


**Fig. 13.** Multidimensional scaling (MDS) plot showing similarities in neuromast number (in 15 superficial neuromast lines on the head) among species of *Elacatinus* and *Tigrigobius* that occupy different microhabitats (see Table 2 and text for additional details). Points were plotted using Euclidean distances (2-D stress value = 0.14) in relation to their similarity/dissimilarity to each other, not with respect to specific values on an axis. This plot indicates that species positioned closer to each other have more similar numbers of superficial neuromasts (or canal neuromast homologs, line u; see Table 2) than those more distant from one another. Green triangle = "coral," dark blue inverted triangle = "other," and light blue square = "sponge." Multiple individuals of the same species are numbered.

tinctions among neuromast subpopulations (which was implied by the way in which the neuromast lines were named by Sanzo, 1911) can be used to identify neuromast homologies among gobies, and among gobiiforms (e.g., apogonids) and others with complex neuromast patterns.

***Ontogeny of neuromast proliferations.***—This study showed that at hatch (0 dph) the number of neuromasts present in *E. lori* (22 neuromasts) is comparable to that in other teleosts including herrings and relatives (Blaxter et al., 1983), zebrafish (*Danio rerio*; Webb and Shirey, 2003), Atlantic croaker (Poling and Fuiman, 1997), and cichlids (Becker et al., 2016). The mechanism of subsequent post-embryonic neuromast proliferation in gobies has not been studied (but is well known on the trunk of zebrafish; Ledent, 2002; Chitnis et al., 2012). However, one might speculate that in order to achieve the high number of superficial neuromasts found in gobies, including *E. lori*, one or more of the following would be necessary: 1) presence of a larger number of lateral line placode-derived primordia from which neuromasts differentiate (see Chitnis et al., 2012), 2) a larger of number neuromasts (e.g., canal neuromast homologs as well as superficial neuromasts) act as founder neuromasts from which new ones may arise via budding (Fig. 6D), and/or 3) superficial neuromast differentiation from primordia and/or proliferation via budding occurs at a higher rate in gobies than in other taxa.

The direction in which neuromast proliferation occurs from a founder neuromast may also help to explain some aspects of the complexity of superficial neuromast patterns in gobies. For instance, the infraorbital canal is absent in *E. lori* (and in other gobies), but some or all of the infraorbital canal neuromast homologs (with hair cell orientation parallel to the ancestral infraorbital canal) may serve as the founder neuromast for each of the tip-to-tip lines of neuromasts radiating from the edge of the orbit (lines 1–7; see Wongrat and Miller, 1991). Another example is the series of vertical lines on the trunk (Fig. 7E) where each may have arisen from a single trunk canal neuromast homolog. Alternatively, each vertical line may consist of a central canal neuromast homolog and superficial neuromasts (of separate origin) dorsal and ventral to it. Whatever the mechanism, these neuromasts appear to comprise a single vertical line with tip-to-tip neuromast organization, but a careful examination of their innervation will be needed to shed light on their origins (see Sato et al., 2019).

A consideration of the direction of proliferation relative to the long axis of the neuromast may also help to explain complex patterns of neuromast proliferation. The generation of a line of neuromasts with a side-by-side arrangement (e.g., canal neuromast homologs or caudal fin neuromasts) would require that additional neuromasts arise from a founder neuromast in a line *parallel* to hair cell orientation but perpendicular to the long axis of the neuromasts. In contrast, generation of a neuromast line with a tip-to-tip arrangement (e.g., superficial neuromast lines) would require that additional neuromasts arise from a founder neuromast and proliferate in a line *perpendicular* to hair cell orientation and parallel to the long axis of the neuromasts. Rouse and Pickles (1991b) had stated that neuromast growth only occurs parallel to hair cell orientation. That argument could be used to predict that neuromast proliferation (e.g., increase in the number of neuromasts in a line) would only occur parallel to hair cell orientation. However, differences in the arrangement of neuromasts *among* lines, even within a species (as in *E. lori*) is evidence that this cannot be the case. This idea is further illustrated by the fact that if the neuromasts comprising the vertical lines on the trunk (Fig. 7E) have a tip-to-tip arrangement and the superficial neuromasts in lines on the caudal fin (Fig. 7F) have a side-by-side arrangement, then a change in the direction of superficial neuromast proliferation is required at the transition from the trunk to the caudal fin. Occasional examples in which the orientation of neuromast lines on the trunk is altered are also instructive. Examination of SEMs of one *E. lori* revealed that despite an aberrant 90° rotation of a single line on the trunk

(from vertical to horizontal), the neuromasts within the line maintained their tip-to-tip arrangement and hair cell orientation relative to the long axis of the neuromasts (unpubl. data). This observation raises interesting questions about how the generation of neuromast shape, maintenance of neuromast arrangement within lines, and neuromast identity (within and among subpopulations) are genetically determined and controlled as neuromasts differentiate and proliferate during the early life history of fishes.

***Functional significance of neuromast size, shape, and arrangements within lines.***—Biomechanical, physiological, and modeling studies of neuromast function have been based on the small, round neuromasts in larval zebrafish (Van Trump and McHenry, 2008; McHenry and Liao, 2014; Yoshizawa et al., 2014) and a small number of other species (Denton and Gray, 1989; van Netten and Kroese, 1989). The functional significance of variation in neuromast shape has not yet been considered, but one can infer that the functional attributes of a diamond-shaped neuromast (length = ~2X width; see above) with a central sensory strip are different from those of round neuromasts of comparable size due to the correlation between the shape of the base of the cupula and the shape of the neuromast (Fig. 6C). In small round neuromasts, an increase in neuromast size should decrease sensitivity due to an increase in cupular stiffness with an increase in hair cell number (McHenry and van Netten, 2007). In most adult fishes, and in the larvae of *E. lori* and other gobies, the hair cells are restricted to a central, oval sensory strip. If the hair cells stiffen the central portion of the cupula only (Rouse and Pickles, 1991b), this may offset the decrease in neuromast sensitivity that occurs as neuromast size and hair cell number increase (M. McHenry, pers. comm.).

Several other factors may contribute to an increase in overall neuromast sensitivity and enhanced spatial resolution of lateral line stimuli by neuromasts in larvae of *E. lori*. The rapid proliferation of neuromasts, as demonstrated here (Figs. 10, 11), should increase the overall sensitivity of the lateral line system to the velocity component of water flows (as opposed to accelerations, which are detected by canal neuromasts; Denton and Gray, 1989). In addition, the shape of neuromasts and their cupulae should also have an effect on neuromast sensitivity (Van Netten and McHenry, 2014). The cupulae of the diamond-shaped neuromasts of *E. lori* have wing-like extensions that reach the tips of the neuromast (Fig. 6A, C). If a flow approaches a neuromast perpendicular to its long axis (e.g., parallel to the axis of best physiological sensitivity of the hair cells), the flow will encounter more surface area than it would if a neuromast of similar size were round with a cylindrical cupula. This would presumably increase the probability of cupular deflection (which generates a neuromast response). In *E. lori*, the small superficial neuromasts within a line share the same shape and hair cell orientation and likely common innervation (as in other gobies; Asaoka et al., 2012, 2014; discussed in Yoshizawa et al., 2010). Furthermore, the dense placement of neuromasts within lines in gobies (Figs. 5E, 7A, B, 12B, D) suggests that they probably do not function in isolation and could provide enhanced spatial resolution for detection of localized water flows (e.g., those generated by small prey or local disturbance or turbulence). Furthermore, when a flow approaches a line of neuromasts with a tip-to-tip arrangement parallel to the axis of best physiological sensitivity of the neuromasts (see Fig. 8C), they would be stimulated simultaneously. However, the same flow approaching a line of neuromasts with a side-by-side arrangement (see Fig. 8B; parallel to the axis of best physiological sensitivity of the neuromasts) would stimulate them sequentially, perhaps with an associated attenuation in stimulus intensity. Thus, the arrangement of neuromasts within a line is likely to contribute to the way in which neuromasts respond to water flows. This suggests that the number, density, and arrangement of small neuromasts within a line as well as the presence of a combination of lines with different neuromast arrangements will enhance the ability of a fish to detect and analyze water flows. It follows that this would provide an advantage for gobies, in particular, especially in low light environments and those in which the hydrodynamic signal to noise ratio is high (e.g., "quiet" hydrodynamic conditions).

On the trunk, the distribution and arrangement of the neuromasts may also enhance their ability to detect flows. In *E. lori*, the neuromasts on the rostral half of the trunk are found in dorsal, lateral, and ventral series, each composed of a small number of short lines of neuromasts (see Figs. 2F, 4). However, most of these neuromasts are under or behind the large pectoral fins when they extend laterally from the body or rest against the body (Fig. 2E). In contrast, neuromasts on the caudal half of the trunk (caudal to the distal end of the pectoral fin) are regularly arranged in a rostro-caudal series of short vertical lines found along the horizontal septum (median series; Fig. 2F) and in three lines on the caudal fin (Fig. 2G), with the axis of best physiological sensitivity in the rostro-caudal axis. This distinction suggests differences in the functional role of the neuromasts in the anterior and posterior portions of the trunk. In particular, we predict that the superficial neuromasts on the caudal half of the trunk detect flows created by the movements of the body and fins during swimming, which would be especially relevant for late-stage pelagic larvae prior to settlement. Superficial neuromasts are known to mediate rheotaxis in adult fishes (Montgomery et al., 2014) and in larval zebrafish in the laboratory (Oteiza et al., 2017), so a proliferation of superficial neuromasts may enhance this ability. However, at the end of the pelagic larval stage, newly transformed gobies (settlers) take up a benthic existence and use their fused pelvic fins (found in most gobiids and gobionellids; Thacker, 2009), which form a sucker disk to attach themselves to a surface. This change in behavior would dramatically change the role of neuromasts in detecting environmental water flows. Furthermore, settlers first attach to the external surface of a tube sponge with their pelvic sucker disk and eventually move into a sponge cavity where they attach to the inner sponge wall (D'Aloia et al., 2011; Majoris et al., 2018a) and are not exposed to environmental flows on the reef. However, it is possible that while living inside tube sponges, *E. lori* can detect changes in the water flows generated by their host sponge (for filter feeding) that occur in response to external conditions (e.g., see Leys et al., 2011). This may allow the fish to indirectly assess external flow conditions that might reflect the availability of planktonic food resources for the fish.

***Ecological correlates of neuromast number.***—Several aspects of morphological variation in the lateral line system are

thought to represent adaptations for enhancement of water flow detection in different behavioral contexts. It has been suggested that a higher number of superficial neuromasts may be adaptive for detection of biologically relevant water flows in environments with low levels of hydrodynamic noise and/or in low light level habitats in which vision is compromised (Coombs and Montgomery, 2014; Webb, 2014a, 2014b; Mogdans, 2019). However, with the exception of work on the surface and cave populations of the Mexican tetra, *Astyanax mexicanus* (Yoshizawa et al., 2010, 2014), attempts to correlate higher numbers of superficial neuromasts with low flow environments among populations within species (Threespine stickleback, *Gasterosteus aculeatus*, Wark and Peichel, 2010; Guppy, *Poecilia reticulata*, Fischer et al., 2013) or among related species (cypriniforms, Beckmann et al., 2010; tripterygiid blennioids, Wellenreuther et al., 2010; pinguipedids, Carton and Montgomery, 2004) have shown variable results.

Among gobies, variation in the morphology of the cranial lateral line canals has been found among populations within a species (a temperate goby, *Eucyclogobius newberryi*; Ahnelt et al., 2004) where more extensively developed canals occur in populations occupying habitats with faster flowing and turbulent waters. Among gobiiform species, higher numbers of neuromasts were found to be associated with enhanced ability to monitor and assess local hydrodynamic flows (e.g., eleotrid gobiiforms, Vanderpham et al., 2016) and the vibratory or acoustic signals produced by mates or competitors (reviewed in Horvatic et al., 2016). On coral reefs, diminutive gobies, a component of the cryptobenthic reef fish fauna (Goatley and Brandl, 2017; Brandl et al., 2018), occupy a range of benthic microhabitats (Patzner et al., 2011). These presumably experience different flow regimes in which the ability to detect flows might benefit from higher or lower numbers of superficial neuromasts. In this case, the superficial neuromast proliferations (as a pre-adaptation or exaptation) may have enabled the repeated invasions of gobies from shallow to mesophotic depths (Tornabene et al., 2016) by providing enhanced prey detection and predator avoidance capabilities under low light conditions.

The current study has demonstrated a correlation between superficial neuromast number in a subset of lines on the head and microhabitat among species of *Elacatinus* and *Tigrigobius* such that the sponge-dwellers examined (planktivorous non-cleaners [Huie et al., 2019]; *E. horsti* and *E. lori*) have significantly more superficial neuromasts than those species living in other microhabitats (Table 2, Fig. 13). This would support the suggestion that sponge-dwellers use their lateral line system to detect planktonic prey and/or may indirectly be able to assess the availability of planktonic prey outside of their sponge hosts. In contrast, the coral-dwellers examined (which tend to be dedicated or facultative cleaners—*E. oceanops*, *E. randalli*, *T. inornatus*, *T. limbaughi* [Huie et al., 2019]) live on the surface of the corals and probably rely more on other sensory systems (e.g., vision, chemoreception) to detect clients (hosts) and the parasites that they consume. Alternatively, the correlation between neuromast number and microhabitat could be explained by the fact that, among species, the degree of lateral line development (canals, superficial neuromast proliferation) is related to fish size. Thus, the smaller number of superficial neuromasts in the smaller coral-dwelling species may be a correlate of their smaller body size and the more limited surface area that can be occupied by neuromasts.

### Conclusions and Suggestions for Further Study

The lateral line system of gobies is notably complex, but the use of a combination of morphological methods to describe neuromast shape and size, the distinctions among three neuromast subpopulations (canal neuromasts, canal neuromast homologs, and superficial neuromasts), the stereotyped neuromast arrangements within lines (tip-to tip, side-by-side), the conserved distribution of neuromast series and lines among closely related species, and a description of the way in which neuromasts develop and proliferate during the larval stage has begun to demystify this complexity. This approach provides a valuable context for further study, especially if combined with the analysis of neuromast innervation patterns.

1) The diamond-shaped neuromasts present in even the youngest larvae of *E. lori* (day-of-hatch) are likely more sensitive than round neuromasts of comparable size due to the larger surface area of their non-cylindrical cupulae. Their functional and behavioral significance during the pelagic larval stage needs to be evaluated. Furthermore, the responses of pelagic larvae to localized and well-defined flow stimuli, e.g., in the context of prey detection and predator avoidance, need to be assessed in order to fully understand the behavior role of neuromasts at all life history stages.
2) The modeling of neuromast function needs to incorporate combinations of size, shape, patterning (e.g., clusters, lines, solitary) and arrangement (e.g., tip-to-tip, side-by-side), and location on body (head, trunk, tail) to more fully predict neuromast function, not only in gobies, but in other taxa with complex neuromast patterns.
3) Finally, the comparison of the number of superficial neuromasts in *Elacatinus* and *Tigrigobius* revealed variation among species that differ in microhabitat on coral reefs. Adaptive evolutionary changes in the morphology of the lateral line system in response to small scale ecological variation within and among species deserves further study.

## DATA ACCESSIBILITY

All raw numerical data are available at: https://www.bcodmo.org/project/651265. Other data are available for study by request directed to the corresponding author.

## ACKNOWLEDGMENTS

We thank our entire Belize field research team (C. Burns, K. Catalano, R. Chaput, C. D'Aloia, J. Ferrito, M. Foretich, R. Francis, F. Francisco, E. Schlatter, and D. Scolaro) who collected and reared gobies in Belize and in Boston. We thank Louie Kerr and his staff at the Central Microscopy Facility at the Marine Biological Laboratory (Woods Hole) for their SEM expertise, Andrew Williston (MCZ, Museum of Comparative Zoology, Harvard University) for his μCT expertise, and Matthew McHenry for discussions of neuromast biomechanics. Zac Tressin and Alec Mauk assisted with μCT reconstructions and histology data collection. Aubree

Jones and Elizabeth Molnar helped with SEM data collection and read earlier versions of the manuscript. This work was done in partial fulfillment of the MS degree awarded to KRN. Funded by NSF grant #1459224 to JFW, NSF #1459546 to PMB, and the George and Barbara Young Chair in Biology at University of Rhode Island to JFW.

## LITERATURE CITED

**Ahnelt, H., J. Göschl, M. N. Dawson, and D. K. Jacobs.** 2004. Geographical variation in the cephalic lateral line canals of *Eucyclogobius newberryi* (Teleostei, Gobiidae) and its comparison with molecular phylogeography. Folia Zoologica 53:385–398.

**Ahnelt, H., and G. Scattolin.** 2003. The lateral line system of a blind goby, *Typhlogobius californiensis* Steindachner, 1879 (Teleostei: Gobiidae). Annalen des Naturhistorischen Museums in Wien 104:11–25.

**Akihito**. 1986. Some morphological characters considered to be important in gobiid phylogeny, p. 629–639. *In*: Indo-Pacific Biology: Proceedings of the Second International Conference on Indo-Pacific Fishes. T. Uyeno, R. Arai, T. Taniuchi, and K. Matsuura (eds.). Ichthyological Society of Japan.

**Asaoka, R., M. Nakae, and K. Sasaki.** 2011. Description and innervation of the lateral line system in two gobioids, *Odontobutis obscura* and *Pterobobius elapoides* (Teleostei: Perciformes). Ichthyological Research 58:51–61.

**Asaoka, R., M. Nakae, and K. Sasaki.** 2012. The innervation and adaptive significance of extensively distributed neuromasts in *Glossogobius olivaceus* (Perciformes: Gobiidae). Ichthyological Research 59:143–150.

**Asaoka, R., M. Nakae, and K. Sasaki.** 2014. Innervation of the lateral line system in *Rhyacichthys aspro*: the origin of superficial neuromast rows in gobioids (Perciformes: Rhyacichthyidae). Ichthyological Research 61:49–58.

**Bassett, D. K., A. G. Carton, and J. C. Montgomery.** 2006. Flowing water decreases hydrodynamic signal detection in a fish with an epidermal lateral-line system. Marine and Freshwater Research 57:611–617.

**Becker, E. A., N. C. Bird, and J. F. Webb.** 2016. Post-embryonic development of canal and superficial neuromasts and the generation of two cranial lateral line phenotypes. Journal of Morphology 277:1273–1291.

**Beckmann, M., T. Erös, A. Schmitz, and H. Bleckmann.** 2010. Number and distribution of superficial neuromasts in twelve common European cypriniform fishes and their relationship to habitat occurrence. International Review of Hydrobiology 95:273–284.

**Bergman, L. M. R.** 2004. The cephalic lateralis system of cardinalfishes (Perciformes: Apogonidae) and its application to the taxonomy and systematics of the family. Unpubl. Ph.D. diss., University of Hawai'i at Mānoa, Honolulu, Hawaii.

**Birdsong, R. S., and C. R. Robins.** 1995. New genus and species of seven-spined goby (Gobiidae: Gobiosomini) from the Offing of the Amazon River, Brazil. Copeia 1995:676–685.

**Blaxter, J. H. S., J. A. B. Gray, and A. C. G. Best.** 1983. Structure and development of the free neuromasts and lateral line system of the herring. Journal of the Marine Biological Association of the United Kingdom 63:247–260.

**Brandl, S. J., C. H. R. Goatley, D. R. Bellwood, and L. Tornabene.** 2018. The hidden half: ecology and evolution of cryptobenthic fishes on coral reefs. Biological Reviews 93:1846–1873.

**Carton, A. G., and J. C. Montgomery.** 2004. A comparison of lateral line morphology of blue cod and torrentfish; two sandperches of the family Pinguipedidae. Environmental Biology of Fishes 70:123–131.

**Chitnis, A. B, D. D. Nogare, and M. Natsuda.** 2012. Building the posterior lateral line system in zebrafish. Developmental Neurobiology 72:234–255.

**Colin, P. L.** 2010. Fishes as living tracers of connectivity in the tropical western North Atlantic: I. Distribution of the neon gobies, genus *Elacatinus* (Pisces: Gobiidae). Zootaxa 2370:36–52.

**Coombs, S., J. Janssen, and J. F. Webb.** 1988. Diversity of lateral line systems: phylogenetic and functional considerations, p. 553–593. *In*: Sensory Biology of Aquatic Animals. J. Atema, R. R. Fay, A. N. Popper, and W. N. Tavolga (eds.). Springer-Verlag, New York.

**Coombs, C., and J. C. Montgomery.** 2014. The role of flow and the lateral line in the multisensory guidance of orienting behaviors, p. 65–102. *In*: Flow Sensing in Air and Water: Behavioural, Neural and Engineering Principles of Operation. H. Bleckmann, J. Mogdans, and S. Coombs (eds.). Springer-Verlag, Berlin.

**D'Aloia, C. C., J. Andres, S. M. Bogdanowicz, A. R. McCune, R. G. Harrison, and P. Buston.** 2020. Unraveling hierarchical genetic structure in a marine metapopulation: a comparison of three high-throughput genotyping approaches. Molecular Ecology 29:2189–2203.

**D'Aloia, C. C., S. M. Bogdanowicz, R. K. Francis, J. E. Majoris, R. G. Harrison, and P. M. Buston.** 2015. Patterns, causes and consequences of marine larval dispersal. Proceedings of the National Academy of Sciences of the United States of America 112:13940–13945.

**D'Aloia, C. C., S. M. Bogdanowicz, R. G. Harrison, and P. M. Buston.** 2014. Seascape continuity plays an important role in determining spatial genetic structure in a coral reef fish. Molecular Ecology 23:2902–2913.

**D'Aloia, C. C., S. M. Bogdanowicz, R. G. Harrison, and P. M. Buston.** 2017. Cryptic genetic diversity and spatial patterns of admixture within Belizean marine reserves. Conservation Genetics 18:211–223.

**D'Aloia, C. C., S. M. Bogdanowicz, J. E. Majoris, R. G. Harrison, and P. M. Buston.** 2013. Self-recruitment in a Caribbean reef fish: a new method for approximating dispersal kernels. Molecular Ecology 22:2563–2572.

**D'Aloia, C. C., J. E. Majoris, and P. M. Buston.** 2011. Predictors of the distribution and abundance of a tube sponge and its resident goby. Coral Reefs 30:777–786.

**D'Aloia, C. C., A. Xuereb, M-J. Fortin, S. M. Bogdanowicz, and P. M. Buston.** 2018. Limited dispersal explains the spatial distribution of siblings in a reef fish population. Marine Ecology Progress Series 607:143–154.

**Denton, E. J., and J. A. B. Gray.** 1989. Some observations on the forces acting on the neuromasts in fish lateral line canals, p. 229–246. *In*: The Mechanosensory Lateral Line: Neurobiology and Evolution. S. Coombs, P. Görner, and H. Münz (eds.). Springer Verlag, New York.

**Faucher, K., A. Aubert, and J.-P. Lagardere.** 2003. Spatial distribution and morphological characteristics of the trunk lateral line neuromasts of the sea bass (*Dicentrarchus labrax*,

L.; Teleostei, Serranidae). Brain, Behavior and Evolution 62: 223–232.

**Feddern, H. A.** 1967. Larval development of the neon goby, *Elacatinus oceanops*, in Florida. Bulletin of Marine Science 17:367–375.

**Fischer, E. K., D. Soares, K. R. Archer, C. K. Ghalambor, and K. L. Hoke.** 2013. Genetically and environmentally mediated divergence in lateral line morphology in the Trinidadian guppy (*Poecilia reticulata*). Journal of Experimental Biology 216:3132–3142.

**Gill, H., and J. Bradley.** 1992. Validation of the use of cephalic lateral-line papillae patterns for postulating relationships among gobioid genera. Zoological Journal of the Linnean Society 106:97–114.

**Goatley, C. H. R., and S. J. Brandl.** 2017. Cryptobenthic reef fishes. Current Biology 27:R452–R454.

**Hoese, D. F., and S. Reader.** 2001. A preliminary review of the eastern Pacific species of *Elacatinus* (Perciformes: Gobiidae). Revista de Biología Tropical 49:157–168.

**Horvatic, S., F. Cavraro, D. Zanella, and S. Malavasi.** 2016. Sound production in the Ponto-Caspian goby *Neogobius fluviatilis* and acoustic affinities within the *Gobius* lineage: implications for phylogeny. Biological Journal of the Linnean Society 117:564–573.

**Hu, Y., J. E. Majoris, P. M. Buston, and J. F. Webb.** 2019. Potential roles of olfaction and taste in the orientation behavior of coral reef fish larvae: Insights from morphology. Journal of Fish Biology 95:311–323.

**Huie, J. M., C. E. Thacker, and L. Tornabene.** 2019. Coevolution of cleaning and feeding morphology in western Atlantic and eastern Pacific gobies. Evolution 74:419–433.

**Janssen, J., S. Coombs, D. Hoekstra, and C. Platt.** 1987. Anatomy and differential growth of the lateral line system of the mottled sculpin, *Cottus bairdi* (Scorpaeniformes: Cottidae). Brain, Behavior and Evolution 30:210–229.

**Jiang, Y., J. Fu, D. Zhang, and Y. Zhao.** 2016. Investigation on the lateral line systems of two cavefish: *Sinocyclocheilus macrophthalmus* and *S. microphthalmus* (Cypriniformes: Cyprinidae). Journal of Bionic Engineering 13:108–114.

**Konagai, M., and M. A. Rimmer.** 1985. Larval ontogeny and morphology of the fire-tailed gudgeon, *Hypseleotris galii* (Eleotridae). Journal of Fish Biology 27:277–283.

**Larson, H. K.** 2011. Systematics of Rhyacichthyidae, p. 51–61. *In*: The Biology of Gobies. R. A. Patzner, J. L. Van Tassell, M. Kovačić, and B. G. Kapoor (eds.). CRC Press, Taylor and Francis Group, Science Publishers, Enfield, New Hampshire.

**Ledent, V.** 2002. Postembryonic development of the posterior lateral line in zebrafish. Development 129:597–604.

**Leys, S. P., G. Yahel, M. A. Reidenbach, V. Tunnicliffe, U. Shavit, and H. M. Reiswig.** 2011. The sponge pump: the role of current induced flow in the design of the sponge body plan. PLoS ONE 6:e27787.

**Lindo, D. P., M. Curcic, C. Paris, and P. M. Buston.** 2016. Description of surface transport in the region of the Belizean Barrier Reef based on observations and alternative high-resolution models. Ocean Modelling 106:74–89.

**Majoris, J. E., K. Catalano, D. Scolaro, J. Atema, and P. M. Buston.** 2019. Ontogeny of larval swimming abilities in three species of coral reef fishes and a hypothesis for their impact on the spatial scale of dispersal. Marine Biology 166:159.

**Majoris, J. E., C. C. D'Aloia, R. K. Francis, and P. M. Buston.** 2018a. Differential persistence favors habitat preferences that determine the distribution of a reef fish. Behavioral Ecology 29:429–439.

**Majoris, J. E., F. A. Francisco, J. Atema, and P. M. Buston.** 2018b. Reproduction, early development, and larval rearing strategies for two sponge-dwelling neon gobies, *Elacatinus lori* and *E. colini*. Aquaculture 483:286–295.

**Marranzino, A. N., and J. F. Webb.** 2018. Flow sensing in the deep sea: the lateral line system of stomiiform fishes. Zoological Journal of the Linnean Society 183:945–965.

**Marshall, N.** 1986. Structure and general distribution of free neuromasts in the Black Goby, *Gobius niger*. Journal of Marine Biological Association of the United Kingdom 66: 323–333.

**McHenry, M. J., and J. C. Liao.** 2014. The hydrodynamics of flow stimuli, p. 73–98. *In*: The Lateral Line System. S. Coombs, H. Bleckmann, R. R. Fay, and A. N. Popper (eds.). Springer, New York.

**McHenry, M. J., and S. M. van Netten.** 2007. The flexural stiffness of superficial neuromasts in the zebrafish (*Danio rerio*) lateral line. Journal of Experimental Biology 210: 4244–4253.

**Meirelles, M. E., M. Y. Tsuzuki, F. F. Ribeiro, R. C. Medeiros, and I. D. Silva.** 2009. Reproduction, early development and larviculture of the barber goby, *Elacatinus figaro* (Sazima, Moura and Rosa 1997). Aquaculture Research 41:11–18.

**Mennesson, M. I., K. Maeda, and P. Keith.** 2019. Evolutionary aspects of cephalic sensory papillae of the Indo-Pacific species of *Eleotris* (Teleostei: Eleotridae). Zoologica Scripta 48:627–639.

**Miller, P.** 1972. Generic status and redescription of the Mediterranean fish *Gobius liechtensteini* Kolombatovic, 1891 (Teleostei: Gobioidea), and its affinities with certain American and Indo-Pacific gobies. Journal of Natural History 6:395–407.

**Miller, P. J., M. Y. El-Tawil, R. S. Thorpe, and C. J. Webb.** 1980. Haemoglobins and the systematic problems set by gobioid fishes, p. 195–233. *In*: Chemosystematics: Principles and Practice. F. A. Bisby, J. G. Vaughan, and C. A. Wright (eds.). Academic Press, London.

**Miller, P. J., and P. Wongrat.** 1979. A new goby (Teleostei: Gobiidae) from the South China Sea and its significance for gobioid classification. Zoological Journal of the Linnean Society 67:239–257.

**Mogdans, J.** 2019. Sensory ecology of the fish lateral-line system: morphological and physiological adaptations for the perception of hydrodynamic stimuli. Journal of Fish Biology 95:53–72.

**Montgomery, J. C., H. Bleckmann, and S. Coombs.** 2014. Sensory ecology and neuroethology of the lateral line, p. 121–149. *In*: The Lateral Line System. S. Coombs, H. Bleckmann, R. R. Fay, and A. N. Popper (eds.). Springer, New York.

**Montgomery, J. C., S. Coombs, and C. F. Baker.** 2001. The mechanosensory lateral line system of the hypogean form of *Astyanax fasciatus*. Environmental Biology of Fishes 62: 87–96.

**Montgomery, J. C., and R. C. Milton.** 1993. Use of the lateral line for feeding in the torrentfish (*Cheimarrichthys fosteri)*. New Zealand Journal of Zoology 20:121–125.

**Mukai, Y., L. L. Chai, S. R. M. Shaleh, and S. Senoo.** 2007. Structure and development of free neuromasts in barramundi, *Lates calcarifer* (Block). Zoological Science 24:829–835.

**Mukai, Y., and L. S. Lim.** 2016. Morphogenesis of free neuromasts in the larvae of brown-marbled grouper *Epinephelus fuscoguttatus*. Marine and Freshwater Behaviour and Physiology 49:159–171.

**Münz, H.** 1989. Functional organization of the lateral line periphery, p. 285–297. *In*: The Mechanosensory Lateral Line: Neurobiology and Evolution. S. Coombs, P. Görner, and H. Münz (eds.). Springer Verlag, New York.

**Nelson, J. S., T. C. Grande, and M. V. H. Wilson.** 2016. Fishes of the World. Fifth edition. John Wiley & Sons, Hoboken, New Jersey.

**Niemiller, M. L., M. E. Bichette, P. Chakrabarty, D. B. Fenolio, A. G. Gluesenkamp, D. Soares, and Y. Zhao.** 2019. Cavefishes, p. 227–236. *In*: Encyclopedia of Caves. Third edition. W. White, D. Culver, and T. Pipan (eds.). Academic Press, Elsevier, London; San Diego, California; Cambridge, Massachusetts; Oxford.

**Oteiza, P., I. Odstrcil, G. Lauder, R. Portugues, and F. Engert.** 2017. A novel mechanism for mechanosensory-based rheotaxis in larval zebrafish. Nature 547:445–448.

**Patzner, R., J. L. Van Tassell, M. Kovačić, and B. G. Kapoor (Eds.).** 2011. The Biology of Gobies. CRC Press, Taylor and Francis Group, Science Publishers, Enfield, New Hampshire.

**Poling, K. R., and L. A. Fuiman.** 1997. Sensory development and concurrent behavioural changes in Atlantic croaker larvae. Journal of Fish Biology 51:402–421.

**Poulson, T. L.** 2001. Adaptations of cave fishes with some comparisons to deep-sea fishes. Environmental Biology of Fishes 62:345–364.

**Puzdrowski, R. L.** 1989. Peripheral distribution and central projections of the lateral-line nerves in goldfish, *Carassius auratus*. Brain, Behavior and Evolution 34:110–131.

**Rouse, G. W., and J. O. Pickles.** 1991a. Ultrastructure of free neuromasts of *Bathygobius fuscus* (Gobiidae) and canal neuromasts of *Apogon cyanosoma* (Apogonidae). Journal of Morphology 209:111–120.

**Rouse, G. W., and J. O. Pickles.** 1991b. Paired development of hair cells in neuromasts of the teleost lateral line. Proceedings of the Royal Society of London B: Biological Sciences 246:123–128.

**Ruber, L., J. L. Van Tassell, and R. Zardoya.** 2003. Rapid speciation and ecological divergence in the American seven-spined gobies (Gobiidae, Gobiosomatini) inferred from a molecular phylogeny. Evolution 57:1584–1598.

**Sanzo, L.** 1911. Distribuzione delle papille cutanee (organi ciatiforme) e suo valore sistematico nei gobi. Mittheilungen aus der Zoologischen Station zu Neapel 20:249–328.

**Sato, M., R. Asaoka, M. Nakae, and K. Sasaki.** 2017. The lateral line system and its innervation in *Lateolabrax japonicus* (Percoidei *incertae sedis*) and two apogonids (Apogonidae), with special reference to superficial neuromasts (Teleostei: Percomorpha). Ichthyological Research 64:308–330.

**Sato, M., M. Nakae, and K. Sasaki.** 2019. Convergent evolution in the lateral line system of Apogonidae (Teleostei: Percomorpha), determined from innervation. Journal of Morphology 280:1026–1045.

**Schindelin, J., I. Arganda-Carreras, E. Frise, V. Kaynig, M. Longair, T. Pietzsch, S. Preibisch, C. Rueden, S. Saalfeld, B. Schmid, J.-Y. Tinevez, D. J. White, V. Hartenstein, K. Eliceiri . . . A. Cardona.** 2012. Fiji: an open-source platform for biological-image analysis. Nature Methods 9: 676–682.

**Schmitz, A., H. Bleckmann, and J. Mogdans.** 2014. The lateral line receptor array of cyprinids from different habitats. Journal of Morphology 275:357–370.

**Soares, D., and M. L. Niemiller.** 2013. Sensory adaptations of fishes to subterranean environments. BioScience 63: 274–283.

**Song, J., and R. G. Northcutt.** 1989. Morphology, distribution and innervation of the lateral-line receptors of the Florida gar, *Lepisosteus platyrhincus*. Brain, Behavior and Evolution 37:10–37.

**Takagi, K.** 1957. Descriptions of some new gobioid fishes of Japan, with a proposition on the sensory line system as a taxonomic character. Journal of the Tokyo University of Fisheries 43:97–126.

**Takagi, K.** 1988. Cephalic sensory canal system of the gobioid fishes of Japan: comparative morphology with special reference to phylogenetic significance. Journal of the Tokyo University of Fisheries 75:499–568.

**Tavolga, W. N.** 1950. Development of the gobiid fish, *Bathygobius soporator*. Journal of Morphology 87:467–492.

**Taylor, M. S., and M. E. Hellberg.** 2005. Marine radiations at small geographic scales: speciation in neotropical reef gobies (*Elacatinus*). Evolution 59:374–385.

**Thacker, C. E.** 2009. Phylogeny of Gobioidei and placement within Acanthomorpha, with a new classification and investigation of diversification and character evolution. Copeia 2009:93–104.

**Thacker, C. E., and D. M. Roje.** 2011. Phylogeny of Gobiidae and identification of gobiid lineages. Systematics and Biodiversity 9:329–347.

**Thacker, C. E., T. P. Satoh, E. Katayama, R. C. Harrington, R. I. Eytan, and T. J. Near.** 2015. Molecular phylogeny of Percomorpha resolves *Trichonotus* as the sister lineage to Gobiodei (Teleostei: Gobiiformes) and confirms the polyphyly of Trachinoidei. Molecular Phylogenetics and Evolution 93:172–179.

**Tornabene, L., J. L. Van Tassell, D. R. Robertson, and C. C. Baldwin.** 2016. Repeated invasions into the twilight zone: evolutionary origins of a novel assemblage of fishes from deep Caribbean reefs. Molecular Ecology 25:3662–3682.

**Valenti, R. J.** 1972. The embryology of the neon goby, *Gobiosoma oceanops*. Copeia 1972:477–482.

**Van Netten, S. M., and A. B. A. Kroese.** 1989. Dynamic behavior and micromechanical properties of the cupula, p. 247–284. *In*: The Mechanosensory Lateral Line: Neurobiology and Evolution. S. Coombs, P. Görner, and H. Münz (eds.). Springer Verlag, New York.

**Van Netten, S. M., and M. J. McHenry.** 2014. The biophysics of the fish lateral line, p. 99–119. *In*: The Lateral Line System. S. Coombs, H. Bleckmann, R. R. Fay, and A. N. Popper (eds.). Springer, New York.

**Van Tassell, J. L.** 2011. A history of gobioid morphological systematics, p. 3–22. *In*: The Biology of Gobies. R. A. Patzner, J. L. Van Tassell, M. Kovačić, and B. G. Kapoor (eds.). CRC Press, Taylor and Francis Group, Science Publishers, Enfield, New Hampshire.

**Van Trump, W. J., and M. J. McHenry.** 2008. The morphology and mechanical sensitivity of lateral line receptors in zebrafish larvae (*Danio rerio*). Journal of Experimental Biology 211:2105–2115.

**Vanderpham, J. P., S. Nakagawa, A. M. Senior, and G. P. Closs.** 2016. Habitat-related specialization of lateral-line system morphology in a habitat-generalist and a habitat-specialist New Zealand eleotrid. Journal of Fish Biology 88: 1631–1641.

**Victor, B. C.** 2014. Three new endemic cryptic species revealed by DNA barcoding of the gobies of the Cayman Islands (Teleostei: Gobiidae). Journal of the Ocean Science Foundation 7:44–73.

**Wark, A. R., and C. L. Peichel.** 2010. Lateral line diversity among ecologically divergent three-spine stickleback populations. Journal of Experimental Biology 213:108–117.

**Watanabe, K., K. Anraku, H. M. Monteclaro, and R. P. Babaran.** 2010. Morphological characteristics of lateral line in three species of fish. Aquaculture Science 58:25–35.

**Webb, J. F.** 2014a. Morphological diversity, development, and evolution of the mechanosensory lateral line system, p. 17–72. *In*: The Lateral Line System. S. Coombs, H. Bleckmann, R. R. Fay, and A. N. Popper (eds.). Springer, New York.

**Webb, J. F.** 2014b. Lateral line morphology and development and implications for the ontogeny of flow sensing in fishes, p. 247–270. *In*: Flow Sensing in Air and Water. H. Bleckmann, J. Mogdans, and S. Coombs (eds.). Springer, Berlin, Heidelberg.

**Webb, J. F., and J. E. Shirey.** 2003. Postembryonic development of the cranial lateral line canals and neuromasts in zebrafish. Developmental Dynamics 228:370–385.

**Wellenreuther, M., M. Brock, J. C. Montgomery, and K. D. Clements.** 2010. Comparative morphology of the mechanosensory lateral line system in a clade of New Zealand triplefin fishes. Brain, Behavior and Evolution 75:292–308.

**Wongrat, P., and P. J. Miller.** 1991. The innervation of head neuromast rows in eleotridine gobies (Teleostei: Gobioidei). Journal of Zoology 225:27–42.

**Yoshizawa, M., S. Goricki, D. Soares, and W. R. Jeffery.** 2010. Evolution of a behavioral shift mediated by superficial neuromasts helps cavefish find food in darkness. Current Biology 20:1631–1636.

**Yoshizawa, M., W. R. Jeffery, S. M. van Netten, and M. J. McHenry.** 2014. The sensitivity of lateral line receptors and their role in the behavior of Mexican blind cavefish (*Astyanax mexicanus*). Journal of Experimental Biology 217: 886–895.